

Design and Synthesis of β -Site Amyloid Precursor Protein Cleaving Enzyme (BACE1) Inhibitors with in Vivo Brain Reduction of β -Amyloid Peptides

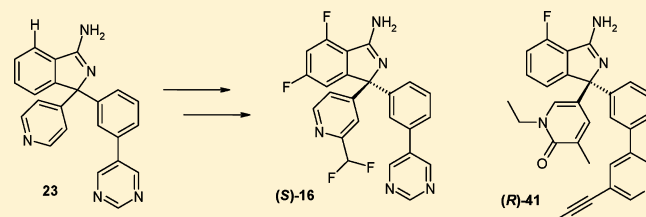
Britt-Marie Swahn,^{*,†} Karin Kolmodin,[†] Sofia Karlström,[†] Stefan von Berg,[†] Peter Söderman,[†] Jörg Holenz,[†] Stefan Berg,[†] Johan Lindström,[†] Marie Sundström,[†] Dominika Turek,[†] Jacob Kihlström,[†] Can Slivo,[†] Lars Andersson,[†] David Pyring,[†] Didier Rotticci,[†] Liselotte Öhberg,[†] Annika Kers,[†] Krisztian Bogar,[†] Fredrik von Kieseritzky,[†] Margareta Bergh,[†] Lise-Lotte Olsson,^{||} Juliette Janson,[§] Susanna Eketjäll,[‡] Biljana Georgievska,[‡] Fredrik Jeppsson,[‡] and Johanna Fälting[‡]

[†]Department of Medicinal Chemistry, [‡]Department of Neuroscience, and [§]Department of Drug Metabolism and Pharmacokinetics (DMPK), AstraZeneca R&D Södertälje, SE-151 85, Södertälje, Sweden

^{||}Discovery Sciences, AstraZeneca R&D Mölndal, SE-43183 Mölndal, Sweden

S Supporting Information

ABSTRACT: The evaluation of a series of aminoisindoles as β -site amyloid precursor protein cleaving enzyme 1 (BACE1) inhibitors and the discovery of a clinical candidate drug for Alzheimer's disease, (S)-32 (AZD3839), are described. The improvement in permeability properties by the introduction of fluorine adjacent to the amidine moiety, resulting in in vivo brain reduction of A β 40, is discussed. Due to the basic nature of these compounds, they displayed affinity for the human ether-a-go-go related gene (hERG) ion channel. Different ways to reduce hERG inhibition and increase hERG margins for this series are described, culminating in (S)-16 and (R)-41 showing large in vitro margins with BACE1 cell IC₅₀ values of 8.6 and 0.16 nM, respectively, and hERG IC₅₀ values of 16 and 2.8 μ M, respectively. Several compounds were advanced into pharmacodynamic studies and demonstrated significant reduction of β -amyloid peptides in mouse brain following oral dosing.

**INTRODUCTION**

Alzheimer's disease (AD) is a neurodegenerative brain disorder characterized clinically by progressive decline of cognitive function, resulting ultimately in death. AD is currently the leading cause of dementia in the elderly and represents a major unmet medical need.¹ Pathologically, AD is characterized by amyloid plaques containing A β peptides² and by neurofibrillary tangles (NFTs) containing hyperphosphorylated τ protein. A β peptides are produced from membrane-bound amyloid precursor protein (APP) by sequential proteolytic cleavage by two aspartyl proteases, β - and γ -secretase. β -Secretase (β -site APP cleaving enzyme, BACE1) has been identified as the enzyme responsible for the initial processing of APP, generating the secreted amino-terminal part of APP (sAPP β) and the membrane-bound carboxy-terminal part C99.³ The C99 fragment is subsequently cleaved by γ -secretase, leading to toxic A β peptides. The generation of C99 and that of A β were found to be blocked in BACE1 knockout mice.⁴ Processes that limit the accumulation of neurotoxic A β peptides are seen to be prospective treatments of AD. Thus, inhibition of BACE1 represents a strategy for the development of disease-modifying therapeutics for the treatment of AD.⁵

Many of the earlier BACE1 inhibitor classes were generated by rational structure-based design of peptidomimetics.

Transition-state isosteres such as statine, homostatine, and hydroxyethylene (HE) were developed into cell-permeable hydroxyethylamine (HEA) isosteres. However, the major drawbacks of these transition-state analogues are high MW, high conformational flexibility, and polar character limiting their ability to cross the blood–brain barrier. Even so, there have recently been reports on HEA isosteres achieving brain A β lowering in animal models.⁶ We have found it to be exceedingly difficult to find BACE1 inhibitor leads using high-throughput screening (HTS), but several compound classes such as acylguanidines,⁷ aminoimidazoles,⁸ and amino-3,4-dihydroquinazolines⁹ have been discovered using this technique. New BACE1 inhibitor leads have also evolved from fragment-based lead generation approaches, resulting in compound classes such as aminohydroxyacetones,¹⁰ 2-aminopyridines,¹¹ dihydroisocytosine,¹² and 2-aminoquinolines.¹³ Despite the large efforts during the past decade to develop BACE1 inhibitors, there are few reports on compounds reducing brain A β peptides in animal models,^{6,13,14} and so far only one report has described

Special Issue: Alzheimer's Disease

Received: June 27, 2012

Published: August 27, 2012

successful BACE1 inhibition in human resulting in reduction of A β levels in lumbar CSF.¹⁵

In this paper, we report the design and synthesis of a potent BACE1 inhibitor series with in vivo brain efficacy. As previously described, fragment-based lead generation resulted in the BACE1 inhibitor lead dihydroisocytosine **1**.¹² This lead was used as a starting point for scaffold hopping into other series such as aminohydantoin **2**,¹⁰ aminoimidazoles **3**,¹⁶ and aminoisindoles **4** as depicted in Figure 1. The aminoisindoles

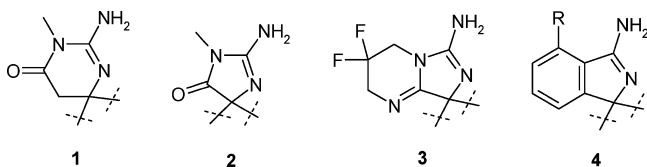


Figure 1. Scaffold hopping from dihydroisocytosines **1** to aminoisindoles **4**.

4 (R = H) were extensively investigated to build SAR information, but the properties of these compounds rendered it not possible to achieve robust in vivo brain efficacy. Herein, we will discuss properties that are important for achieving in vivo brain effects and describe the efforts to improve aminoisindole derivatives **4** to attain reduction of β -amyloid peptides in the brain.

We were able to pinpoint the reason for the lack of in vivo effects in the brain to the characteristics of the amidine moiety. The properties of the amidine group could be modulated via the introduction of a substituent (R = F) ortho to the amidine group, resulting in several novel BACE1 inhibitors with enhanced permeability properties and potential to reduce the A β peptide levels in the mouse brain. The BACE1 potency of this fluoroaminoisindole series **4** (R = F) was further improved and reached subnanomolar levels. These basic compounds also displayed affinity for the human ether-a-go-go related gene (hERG)-encoded potassium ion channel, which is involved in cardiac repolarization. Inhibition of the hERG current may cause QT interval prolongation. Drug-induced QT prolongation increases the likelihood of a polymorphous

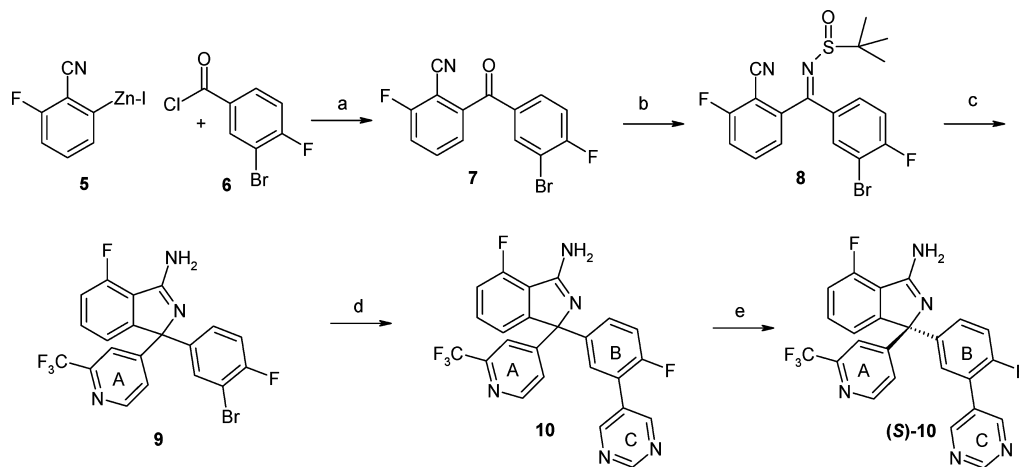
ventricular arrhythmia known as *Torsades de Pointes* (TdP), which may evolve into ventricular fibrillation and sudden death.¹⁷ A number of drugs have been withdrawn from late-stage clinical trials and the market due to these cardiotoxic effects; therefore, it is important to identify hERG inhibitors early in drug discovery.¹⁸ Different approaches to avoid hERG side effects for the fluoroaminoisindole series are discussed.

CHEMISTRY

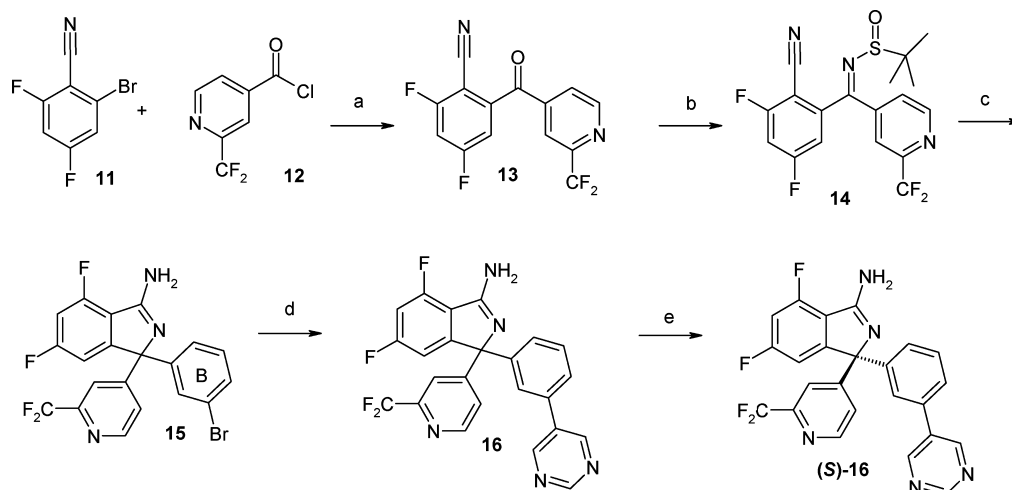
The syntheses of the compounds disclosed in this paper follow the descriptions summarized in Schemes 1–4. The majority of compounds were synthesized using method A (Scheme 1), where the A-ring (as defined in Scheme 1) and a sulfinimide were reacted in the cyclization step. Commercially available phenylzinc(II) iodide **5** was coupled with acid chloride **6** using a palladium catalyst to yield the ketone **7**. The ketone was converted into the corresponding sulfinimide **8** using titanium ethoxide and 2-methyl-2-propanesulfinamide. It was found crucial to lithiate the corresponding pyridine (A-ring) and add the sulfinimide **8** to the lithiated species at very low temperatures to retrieve reasonable yields of the cyclized compound **9**. In the final synthetic step, the (C-ring) pyrimidine was introduced by a palladium-catalyzed Suzuki¹⁹ reaction to give racemate **10**. The most active BACE1 enantiomer (*S*)-**10** was isolated by chiral preparative supercritical fluid chromatography (SFC).

In some cases the lithiation of pyridines failed, due to base-labile substituents, and method B shown in Scheme 2 was used. The difluorophenylzinc(II) bromide reagent was prepared by treating bromide **11** with Rieke zinc. Subsequent addition of the reagent to the acid chloride **12** in the presence of CuCN and LiCl produced the ketone **13**. The ketone was converted into the corresponding sulfinimide **14** using titanium ethoxide and 2-methyl-2-propanesulfinamide. 1,3-Dibromobenzene was lithiated with *n*-butyllithium and added to the sulfinimide **14** at low temperature to yield cyclized intermediate **15**. A palladium-catalyzed Suzuki coupling with 5-pyrimidinylboronic acid gave racemate **16**, which was separated using chiral chromatography to yield the enantiomerically pure (*S*)-**16**.

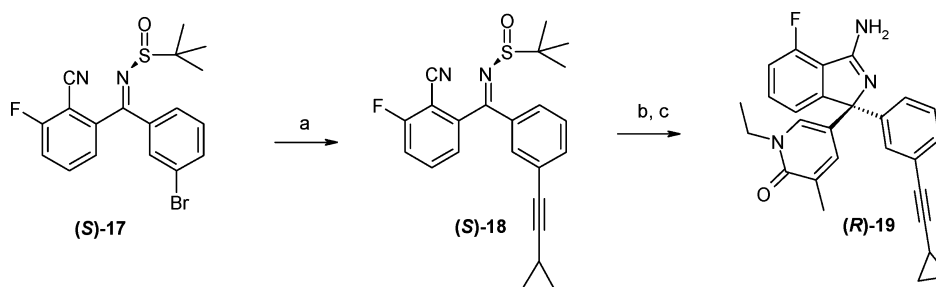
Scheme 1. General Synthesis Method A^a



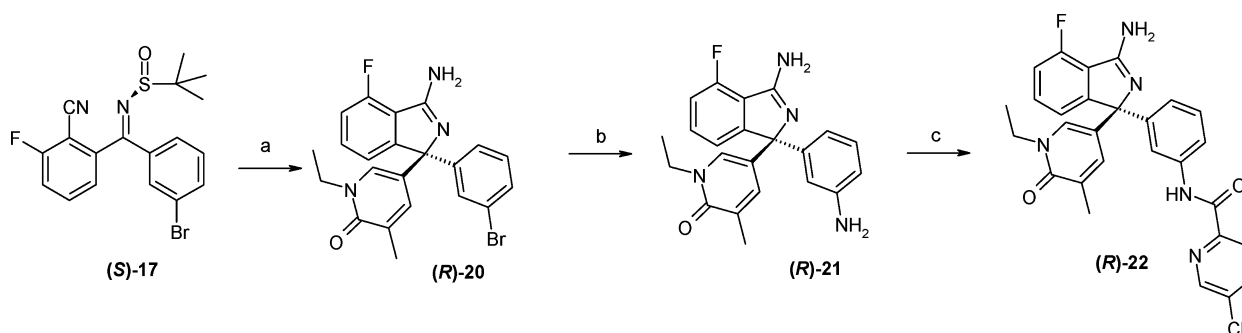
^aReagents and conditions: (a) tetrakis(triphenylphosphine)palladium(0), THF, 0 °C; (b) Ti(OEt)₄, THF, 2-methyl-2-propanesulfinamide, reflux; (c) *t*-BuLi (1.6 M in pentane), THF, -100 °C, 4-bromo-2-(trifluoromethyl)pyridine; (d) 5-pyrimidinylboronic acid, DMF, 90 °C, Pd^{II}Cl₂dppf·CH₂Cl₂, aqueous K₂CO₃; (e) Chiralpak AD column (21.2 × 250 mm), eluent IPA (0.1% DEA)/CO₂ (20:80).

Scheme 2. General Synthesis Method B^a

^aReagents and conditions: (a) Rieke zinc, THF, CuCN, LiCl, rt; (b) Ti(OEt)₄, 2-methylpropane-2-sulfinamide, THF, 60 °C; (c) *n*-BuLi, 1,3-dibromobenzene, THF, -78 °C; (d) 5-pyrimidinylboronic acid, PdCl₂(PPh₃)₂, DME/EtOH/H₂O (3:2:1), K₂CO₃, 100 °C; (e) Chiralpak AD column (21.2 × 250 mm), eluent IPA (0.1% DEA)/CO₂ (15:85).

Scheme 3. Synthesis of Alkyne Derivative (*R*)-19^a

^aReagents and conditions: (a) copper(I) iodide, bis(triphenylphosphine)palladium(II) chloride, 2-methyltetrahydrofuran, ethynylcyclopropane, Et₃N, 60 °C; (b) *n*-BuLi (2.5 M in hexanes), butylmagnesium chloride (2 M in THF), 5-bromo-1-ethyl-3-methylpyridin-2(1H)-one, THF, -40 °C; (c) Chiralpak AD column (21.2 × 250 mm) eluent IPA (0.1% DEA)/*n*-heptane (10:90).

Scheme 4. Synthesis of Amide Analogue (*R*)-22^a

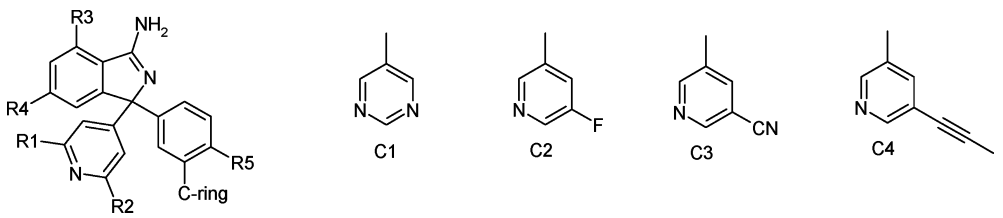
^aReagents and conditions: (a) *n*-BuLi, *n*-butylmagnesium chloride, 5-bromo-1-ethyl-3-methylpyridin-2(1H)-one, THF, -25 °C; (b) *trans*-4-hydroxy-L-proline, copper(I) iodide, K₂CO₃, DMSO, NH₃ (32% in H₂O), microwave reactor, 110 °C; (c) 5-chloropicolinic acid, 1-(3-(dimethylamino)propyl)-3-ethylcarbodiimide hydrochloride, DCM, DMF, 0 °C.

We found that it was possible to obtain chiral induction in the cyclization step in Schemes 1 and 2 by using enantiomerically pure sulfinimides. The commercially available (*S*)-2-methyl-2-propanesulfinamide was used to prepare enantiomerically enriched sulfinimide (*S*)-17, applying the same procedure as described for 8 and 14. The palladium-catalyzed coupling of (*S*)-17 with ethynylcyclopropane to yield intermediate (*S*)-18 was performed before the cyclization step (Scheme 3).

Cautious treatment of 5-bromo-1-ethyl-3-methylpyridin-2(1H)-one with butyllithium followed by subsequent addition of intermediate (*S*)-18 gave (*R*)-19 with an enantiomeric purity of 70%. The pure (*R*)-19 enantiomer was isolated after chiral HPLC chromatography.

(*S*)-17 was also used as a starting material in the synthesis of the amide derivative (*R*)-22 (Scheme 4). Addition of (*S*)-17 to metalated 5-bromo-1-ethyl-3-methylpyridin-2(1H)-one gave

Table 1. Fluoroaminoisoindoles with Pyridine as the Trp76 Hydrogen Bond Acceptor



compd	R1	R2	R3, R4, R5	C-ring	IC ₅₀ (FRET) ^a (nM)	IC ₅₀ (cell sAPPβ) ^a (nM)	P _{app} ^b (10 ⁻⁶ cm/s)	efflux ratio ^c	IC ₅₀ (hERG) ^d (μM)	CL _{int} ^e (μL/min/10 ⁶ cells)	pK _a ^f	eLogD ^g
23	H	H	H, H, H	C1	500	90.3	3.4	12	16	11.7	8.4	0.7
24	CF ₃	H	H, H, H	C1	134	2.10	0.13	>10	5.5	5.2	nd ^h	2.3
25	H	H	F, H, H	C1	158	11.4	12	3.1	5.7	16	7.1	0.9
(S)-25	H	H	F, H, H	C1	124	8.25	22	1.9	3.1	13.7	7.2	1.1
26	H	H	F, H, H	C2	137	25.6	24	0.7	1.6	14.1	7.1	2.0
27	CF ₃	H	F, H, H	C1	241	43.1	39	0.6	11	10.6	6.9	2.7
28	CF ₃	H	F, H, H	C3	253	29.9	16	0.8	1.7	5.2	nd	3.7
10	CF ₃	H	F, H, F	C1	198	29.3	25	1.0	16	6.9	6.4	3.0
(S)-10	CF ₃	H	F, H, F	C1	125	22.1	30	0.9	7.9	10.0	nd	3.0
29	CH ₃	CH ₃	F, H, H	C1	1380	10.7	19	2.2	6.4	5.6	8.0	1.4
30	cyclopropyl	H	F, H, H	C1	86.4	18.4	42	0.5	3.5	27.6	7.4	2.1
31	OCH ₃	H	F, H, H	C1	401	21.5	21	1.2	2.2	42.0	7.1	2.0
32	CF ₂	H	F, H, H	C1	42.8	17.0	27	1.2	7.2	27.5	6.8	2.0
(S)-32	CF ₂	H	F, H, H	C1	35.1	16.7	34	0.9	4.8	20.9	7.1	2.0
(S)-16	CF ₂	H	F, F, H	C1	36.2	8.64	37	0.9	19	40.4	6.2	2.3
33	CF ₂	H	F, H, H	C4	6.49	2.97	4.7	2.3	2.9	19.8	nd	3.9

^aIC₅₀ values are the means of at least two experiments. ^bP_{app} is the measured permeability (apical (A) to basolateral (B)) through Caco-2 cells. ^cThe efflux ratio is P_{app}(B-A)/P_{app}(A-B) in Caco-2 cells. ^dMeasured in hERG-expressing CHO cells using IonWorks technology. ^eMetabolic stability in rat hepatocytes. ^fDetermined by pressure-assisted capillary electrophoresis. ^gDetermined by reversed-phase liquid chromatography. ^hnd = not determined.

enantiomerically enriched (*R*)-**20** which was further purified by chiral chromatography. Treatment of the bromide (*R*)-**20** with copper iodide and ammonia yielded the corresponding amine (*R*)-**21**. Standard amide coupling reaction with 5-chloropicolinic acid and (*R*)-**21** afforded the corresponding amide (*R*)-**22**.

RESULTS AND DISCUSSION

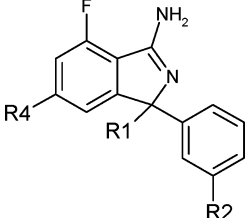
The synthesized compounds were evaluated for BACE1 inhibition in a fluorescence resonance energy transfer (FRET) protocol using the soluble part of the human β-secretase (aa1–aa460) and substrate (europium)-CEVNLDAEFK(Qsy7). The cell-based assay for BACE1 inhibition used specific antibodies to monitor reduction of sAPPβ release from human neuronal-derived SH-SY5Y cells. Measured properties such as Caco-2 permeability, efflux, and metabolic stability, which are important for the selection of candidates to be evaluated in vivo, are shown in Tables 1 and 2. The disclosed compounds are divided into two tables mainly due to the different properties emanating from the A-rings (as defined in Scheme 1), but also illustrating the development history of this series.

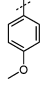
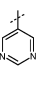
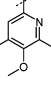
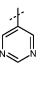
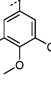
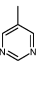
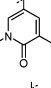
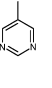
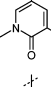
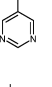
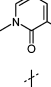
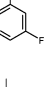
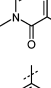
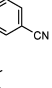
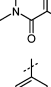
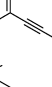
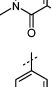
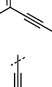
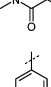
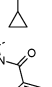
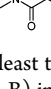
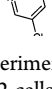
As previously described, we have been able to soak different inhibitors into crystals of BACE1.¹⁶ The crystal structure of compound **10** bound in BACE1 was refined to 1.79 Å resolution (Figure 2). The X-ray structure shows that the amidine group of the ligand interacts with residues Asp32 and Asp228, in analogy with related aminoimidazole and amino-hydantoin structures.^{16,20} The A-ring is located close to the S2' region and fills the pocket occupied by Tyr71 in the peptide-bound, flap-closed conformation of BACE1.²¹ A hydrogen

bond acceptor in the para position of the A-ring, such as a pyridine nitrogen or a methoxy substituent, makes an important interaction with Trp76 in this open conformation. A substituent ortho to the acceptor may either fill a subpocket in the enzyme or prefer to be oriented toward the exposed side of the ring, facing the flap. A trifluoromethyl group ortho to the pyridine nitrogen as in **10** fills the subpocket and displaces a conserved water molecule normally coordinated by the backbone of Asn37 and the side chain of Ser35. The B-ring (defined in Scheme 1) is placed in the hydrophobic S1 pocket, and the B-ring *p*-fluoro substituent is small enough to fit into S1 close to residues Phe108–Ile110. The C-ring (defined in Scheme 1) occupies the S3 pocket, and both pyrimidine nitrogens coordinate one water molecule each. One of these waters is buried in the S3 subpocket and interacts with Ser229, thereby bridging the interaction between the protein and the inhibitor. The enantiomeric preference for compound **10** would be the (*S*)-enantiomer as apparent from the crystal structure (Figure 2) and in line with discussions by Malamas et al.^{8,20} The cell IC₅₀ value was determined to be 22 nM for (*S*)-**10** and 7000 nM for (*R*)-**10**.

A fluoro substituent ortho to the amidine in the isoindole core leads to formation of a weak internal H-bond and reduced pK_a as shown for **23** compared to **25** (Table 1). Calculations also show that the solvation energy is less negative for the *o*-fluoro-substituted compound, as compared to fluoro in the meta or para position (data not shown). The combination of electronic and steric effects results in “shielding” of the polar exocyclic nitrogen from the solvent. In practice, less than two H-bond donors are seen by the environment and permeability

Table 2. Fluoroaminoisoindoles with Methoxy or Pyridone as the Trp76 Hydrogen Bond Acceptor



Comp	R1	R2	R4	IC ₅₀ nM FRET ^a	IC ₅₀ nM cell sAPP ^β ^b	P _{app} (10 ⁻⁶ cm/sec) ^b	Efflux ratio ^c	IC ₅₀ μM hERG ^d	Cl _{int} (μL/min/ 10 ⁶ cells) ^e	pK _a ^f	eLogD ^g
34			H	135	12.5	12	1.1	0.5	40.3	8.2	2.4
35			H	78.5	2.92	33	0.5	3.8	25.3	8.1	2.7
36			H	41.7	3.40	23	0.6	2.1	30.9	nd	3.1
37			H	60.8	11.4	1.7	17	>33	6.9	7.4	0.9
38			H	15.5	9.09	3.7	10	15	9.3	7.7	1.3
39			H	12.9	3.98	9.8	3.5	2.7	15.3	nd	2.4
40			H	8.26	1.84	5.1	8.4	nd	6.5	nd	nd
(R)- 41			H	2.44	0.16	11	1.0	2.8	15.6	7.5	3.0
(R)- 42			F	2.59	0.38	8.9	0.7	3.1	6.4	nd	3.4
(R)- 19			H	6.08	0.76	12	0.9	8.5	54.1	7.6	3.6
(R)- 22			H	2.49	0.15	9.3	2.6	1.3	<5	7.3	3.0

^aIC₅₀ values are the means of at least two experiments. ^bP_{app} is the measured permeability (apical (A) to basolateral (B)) through Caco-2 cells. ^cThe efflux ratio is P_{app}(B-A)/P_{app}(A-B) in Caco-2 cells. ^dMeasured in hERG-expressing CHO cells using IonWorks technology. ^eMetabolic stability in rat hepatocytes. ^fDetermined by pressure-assisted capillary electrophoresis. ^gDetermined by reversed-phase liquid chromatography. ^hnd = not determined.

and efflux are improved, as evident when comparing compounds **23** with **25** and compounds **24** with **27**. The introduction of the *o*-fluoro substituent was well tolerated, and for compound **25** compared to **23**, the potency was increased in the FRET assay from 500 to 158 nM. The fluoro substituent is nicely pentacoordinated by water and side chain oxygen atoms in the X-ray structure. The O–F distances range from 2.9 to 3.3 Å.

The racemic compound **25** was separated into its enantiomers. Interestingly, the most active BACE1 enantiomer (*S*)-**25** displayed improved permeability and efflux properties.

This trend seemed to be general and can be noticed when comparing compound **10** with (*S*)-**10** and **32** with (*S*)-**32**. Unfortunately, affinity for the hERG ion channel also increased. For the most active BACE1 enantiomers (*S*)-**10**, (*S*)-**25**, and (*S*)-**32**, the hERG IC₅₀ values were reduced by a factor of 2 compared to those of the racemates. Thus, enantiomer separation resulted in a larger effect on hERG affinity than on BACE1 affinity.

The two most common ways of reducing hERG affinity are to lower pK_a or lipophilicity.²² The introduction of a trifluoromethyl group as in **27** reduced the pK_a and resulted

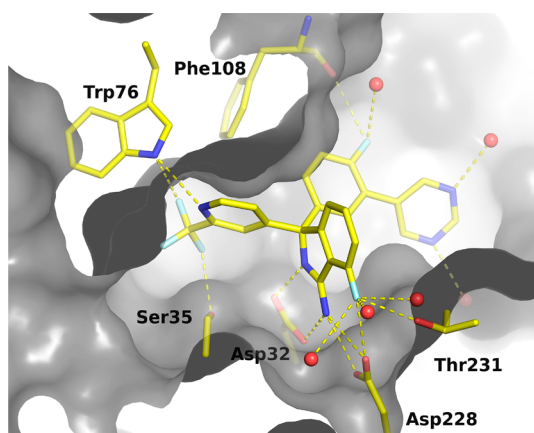


Figure 2. Crystal structure of compound **10** in complex with BACE1. Key interactions between inhibitor (yellow), protein amino acid residues (yellow), N (blue), O (red), F (light blue), and water molecules (red spheres) are highlighted with dashed lines. The protein surface is depicted in gray (residues 72–73 in the flap region are not shown for clarity). The data collection and refinement statistics are summarized in Table 3.

in lower hERG affinity as evident by comparing compound **25** with **27**, but the BACE1 affinity was also reduced. Lipophilicity was experimentally determined as eLogD values in a method using reversed-phase liquid chromatography to estimate $\log D$ on the basis of the compound retention time.²⁹ In the fluoroaminoisindole series we noticed that an eLogD value below 1.5 increased the efflux ratios, which would be

detrimental for reaching high brain concentrations. Thus, we concentrated on designing compounds with a predicted $\log D$ of above 1.5 but also below 3.5 to avoid issues associated with high lipophilicity.²³ To improve BACE1 potency of the (trifluoromethyl)pyridine **27**, we investigated if the 5-cyano-3-pyridinyl C-ring previously found to increase affinity would be useful. The BACE1 inhibition in human neuronal-derived SH-SY5Y cells was increased comparing compound **28** with **27**; however, hERG affinity was increased even more. Another C-ring previously indicating increased affinity was the 5-fluoro-3-pyridinyl, but as evident from compound **26** it did not display increased cell potency in this series.

The 4-pyridinyl analogue (*S*)-**25** with a BACE1 potency in the cell assay of 8.25 nM was a potent CYP inhibitor, which is a common issue for ortho-unsubstituted 4-pyridinyls.²⁴ On the other hand, the (trifluoromethyl)pyridinyl compound **27** with reduced CYP affinity displayed good properties for Caco-2 permeability, efflux, and metabolic stability in rat hepatocytes. We therefore decided to synthesize **10** with the additional fluoro substituent in the para position of the B-ring. We envisioned that the fluorine could fit into a small subpocket, and indeed, the BACE1 cell potency increased to an IC_{50} value of 29 nM and hERG affinity decreased to an IC_{50} value of 16 μM .

Other substituents on the pyridine A-ring were examined, and both the cyclopropyl **30** and methoxy **31** compounds were more potent than the trifluoromethyl analogue **10** in the cell assay. However, the pK_a was increased, which resulted in unfavorable hERG affinity. The dimethyl compound **29** was even more potent in the cell assay, but here we could notice a

Table 3. X-ray Crystallography Data Collection and Refinement Statistics

	BACE1 complex with 10	BACE1 complex with (<i>R</i>)- 41
	Data Collection	
space group	$P2_12_12_1$	$P2_12_12_1$
unit cell dimensions	$a = 47.54 \text{ \AA}$, $b = 76.39 \text{ \AA}$, $c = 104.34 \text{ \AA}$ $\alpha = 90.0^\circ$, $\beta = 90.0^\circ$, $\gamma = 90.0^\circ$	$a = 47.96 \text{ \AA}$, $b = 75.91 \text{ \AA}$, $c = 104.65 \text{ \AA}$ $\alpha = 90.0^\circ$, $\beta = 90.0^\circ$, $\gamma = 90.0^\circ$
resolution range ^a (Å)	35.87–1.79 (1.84–1.79)	43.08–1.83 (1.93–1.83)
no. of observations	125330	101856
no. of unique reflns	36601	34330
data redundancy ^a	3.4 (3.4)	3.0 (2.9)
data completeness (%) ^a	99.9 (100.0)	99.6 (99.8)
$\langle I/\sigma(I) \rangle$ ^a	20.6 (4.5)	15.0 (2.1)
R_{merge} ^a (%)	4.0 (25.7)	5.1 (45.2)
	Refinement	
resolution range ^a (Å)	35.87–1.79 (1.84–1.79)	43.08–1.83 (1.89–1.83)
R_{work} ^a (%)	17.6 (26.4)	17.3 (24.0)
R_{free} ^a (%)	21.0 (31.4)	22.6 (27.7)
Wilson <i>B</i> -factor (Å ²)	22.0	23.0
overall mean <i>B</i> -factor (Å ²)	25.1	26.6
no. of atoms		
protein atoms	2983	2974
heterogen atoms	449	416
solvent atoms	402	364
rmsd values		
bond lengths (Å)	0.010	0.010
bond angles (deg)	1.12	1.14
Ramachandran statistics (%) (PROCHECK) ³³		
most favored + add. allowed	99.7	100
generously allowed	0.3	0

^aNumbers in parentheses refer to the highest resolution shell.

very large increase in potency in going from FRET to cell assay. This increase in potency is a common feature for the more basic inhibitors ($pK_a > 6$),²⁵ but for **29** there could be additional factors involved.

A closer examination of the crystal structure of compound **10** revealed that the trifluoromethyl group seemed to be too large for the S2' subpocket as one of the fluorine atoms apparently clashed with the BACE1 protein surface. The cyclopropyl and methoxy groups fit better, but the methoxy compound **31** showed poor metabolic stability and the cyclopropyl compound **30** displayed unfavorable hERG affinity. Instead, we decided to try a difluoromethyl group to keep the pK_a low and at the same time achieve a better fit in the S2' subpocket. In particular, the IC_{50} value in the FRET assay improved from 241 to 43 nM when replacing the trifluoromethyl substituent in **27** with the difluoromethyl group in **32**. Compound **32** was separated into its enantiomers, and (*S*)-**32** showed promising in vitro properties for BACE1 inhibition in the cell assay with an IC_{50} value of 16.7 nM, resulting in a 280-fold margin to the hERG IC_{50} (4.8 μ M). The permeability and efflux values were good, indicating that high brain/plasma ratios could be achieved. Compound (*S*)-**32**, with an oral bioavailability in mice of 73% and an oral half-life of 1.5 h, was selected as a preclinical candidate drug and therefore extensively studied in animal models for A β 40 reduction and for evaluation of margins to hERG side effects. Blockade of the human hERG channel and QT prolongation have become surrogate markers of potential cardiotoxicity of pharmaceutical compounds. In preclinical studies, the hERG assay is widely used as a first indication for a potential effect of compounds on IKr conduction. However, even though a safety margin can be predicted from these values, it is difficult to quantitatively predict the actual level of QT prolongation expected in vivo in preclinical studies and in human. Thus, these findings need to be followed up in an in vivo setting such as in the guinea pig monophasic action potential (MAP) assay and/or in vivo dog electrocardiogram (ECG) recordings. Compound (*S*)-**32** was designated clinical candidate AZD3839 and progressed to further in vivo preclinical and clinical testing (a detailed account of these studies will be published elsewhere by Falting et al.).

We wanted to explore if the in vitro hERG margins could be improved, and the most promising way would be to reduce pK_a for these pyridine analogues. An additional fluoro substituent para to the amidine moiety in the isoindole core structure was predicted to result in decreased pK_a , and compound (*S*)-**16** displayed the lowest hERG affinity in this series with an IC_{50} value of 19 μ M and a pK_a of 6.2. The BACE1 cell potency was increased to an IC_{50} value of 8.6 nM, resulting in a 2200-fold margin to the hERG IC_{50} .

The compounds with methoxy as the hydrogen bond acceptor interacting with Trp76 were potent BACE1 inhibitors (Table 2). This indicated that the geometric constraints of the BACE1 protein and the inhibitor govern the affinity rather than the hydrogen bond acceptor strength of the substituent on the inhibitor. The pyridine analogue **25** was slightly less potent in the FRET assay compared to methoxy analogue **34** (Table 2) in contrast to what could be expected when comparing the hydrogen bond acceptor strengths of these groups.³⁰ The *p*-methoxy ortho-disubstituted A-rings displayed high BACE1 affinity, and compounds **35** and **36** with cell IC_{50} values of 2.9 and 3.4 nM, respectively, achieved high margins to hERG. The permeability and efflux properties were good for the methoxy

analogues **34**, **35**, and **36**, but the methoxy group was a metabolic weak spot and contributed to CYP inhibition.

Another option to increase margins to hERG besides decreasing affinity for hERG would be to increase affinity for BACE1, and we anticipated that increasing the hydrogen bond acceptor strengths of the hydrogen acceptors on or in the A-ring should result in increased BACE1 inhibition. Thus, pyridone was tried as a replacement for the methoxyphenyl A-ring. Compound **37** was reasonably potent, but the desolvation energy cost of the pyridone moiety probably reduced some of the expected increase in affinity. This group displayed reduced permeability and increased efflux, but metabolic stability was considerably improved compared to those of the methoxyphenyl compounds **34**, **35**, and **36**. The improved metabolic stability of the pyridones was also translated into excellent bioavailability in mouse and rat. Elongating the methyl into ethyl as in **38** improved the FRET potency considerably. We sought improved permeability and efflux properties, and since the pyridones **37** and **38** were quite polar with $\log D$ values of 0.9 and 1.3, respectively, we decided to explore more lipophilic C-rings. Both the 5-fluoro-3-pyridinyl and 5-cyano-3-pyridinyl compounds **39** and **40** increased BACE1 inhibition in the FRET and cell assays, but the efflux ratio was still high (>1.5).

The 5-propynyl-3-pyridinyl analogue (*R*)-**41** with additionally increased lipophilicity displayed reduced efflux and reasonable permeability in Caco-2 cells. (*R*)-**41** was very potent in the BACE1 cell assay with an IC_{50} value of 0.16 nM, resulting in a high (>10000-fold) margin to the hERG IC_{50} . (*R*)-**41** displayed excellent in vivo pharmacokinetic (PK) properties, with an oral bioavailability in mice of 100% and per os (po) half-life of 2.3 h, and was extensively studied in animal models for A β 40 reduction. A detailed account of these studies will be published elsewhere by Falting et al.

The introduction of a fluoro substituent para to the amidine group as in compound (*R*)-**42** did not result in reduced affinity for hERG and increased BACE1 potency, a result contrary to what was expected when comparing this compound to compound (*S*)-**16**.

The crystal structure of compound (*R*)-**41** bound to BACE1 was refined at 1.83  resolution (Figure 3). The amidine interacts with the two aspartic acids as with compound **10** in Figure 2. The carbonyl of the pyridone ring interacts with Trp76 via a hydrogen bond and is further coordinated by a water molecule, forming a novel network of protein–water interactions as compared to the pyridinyls and methoxy-substituted phenyls.^{16,20,31} The methyl substituent next to the carbonyl is oriented into the protein, whereas the ethyl group is solvent exposed. In general, the orientation of the A-ring has been difficult to predict by molecular modeling, and thus, X-ray crystallography has been an important technique to support the design of new inhibitors. The C-ring propynyl protrudes into the S3 subpocket and displaces the water observed in the BACE1–**10** complex (Figure 2). This in turn induces a conformational change of the so-called 10s loop defined by residues 9–14.³²

The 5-propynyl-3-pyridinyl C-ring with its unique binding into the S3 subpocket was also explored in the pyridinyl subseries. Compound **33** (Table 1) was synthesized, and indeed, it enhanced BACE1 potency in this subseries, but unfortunately, permeability properties deteriorated and hERG affinity increased.

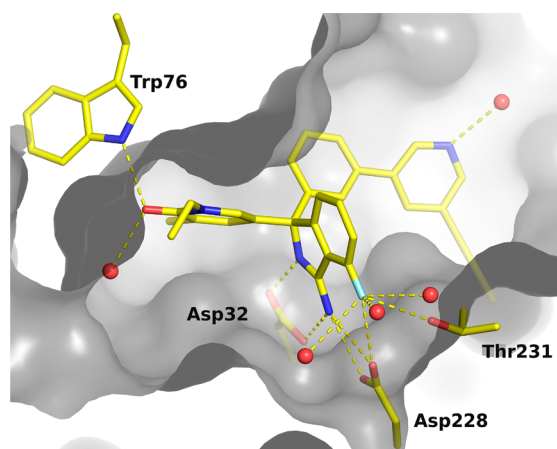


Figure 3. Crystal structure of compound (R)-41 in complex with BACE1. Key interactions between inhibitor (yellow), protein amino acid residues (yellow), N (blue), O (red), F (light blue), and water molecules (red spheres) are highlighted with dashed lines. The protein surface is shown in gray (residues 72–73 in the flap region are not shown for clarity). The data collection and refinement statistics are summarized in Table 3.

Substituents other than aromatic C-rings could be used to reduce the molecular weight and polar surface area, resulting in improved permeability properties as we have previously described.¹⁶ A representative example for these analogues is (R)-19, but in the pyridone subseries the effect on permeability was at most minor when comparing (R)-41 with (R)-19. The cyclopropylethynyl compound (R)-19 was found to be surprisingly potent in the BACE1 cell assay with an IC_{50} value of 0.76 nM, indicating that the aromatic C-rings were probably not the optimal binding component in the S3 pocket. This assumption was also evident when comparing compound (R)-22 with 39 or 40, where the elongated compound (R)-22 displayed about a 10-fold increase in potency in the BACE1 cell assay, reaching an IC_{50} value of 0.15 nM. When examining the crystal structure of an analogue closely related to (R)-22 in complex with BACE1, we could see a hydrogen bond interaction between the amide NH and the backbone carbonyl of Gly230. This H-bond interaction probably explained the increase in affinity for (R)-22.

Both BACE1 and γ -secretase mediate cleavage of many substrates involved in cell signaling, and it is crucial to sustain these pathways while altering the $A\beta$ formation. For γ -secretase inhibitors, a major liability has been interference with the Notch

signaling pathway, critical in proliferative signaling during neurogenesis. All fluoroaminoisindole compounds tested in a Notch assay (not shown) are inactive, and thus, these compounds are not believed to interfere with γ -secretase-related signaling. The fluoroaminoisindoles were also tested for selectivity against BACE2, and data for representative compounds are shown in Table 4.

(S)-25 was the first synthesized compound in our in-house chemical series that produced a robust and statistically significant lowering of β -amyloid peptides in vivo. The incorporation of a fluoro adjacent to the amidine moiety had a large impact on the ability of the series to reduce $A\beta_{40}$ in the brain. The reason for the in vivo effect is most likely explained by the improved permeability and efflux properties of the fluoroaminoisindoles. Several compounds from the fluoroaminoisindole series were evaluated in vivo, and they all displayed the ability to lower the $A\beta_{40}$ levels in the brain of C57BL/6 mice, as shown in Table 4. Furthermore, all fluoroaminoisindoles tested in vivo reduced the levels of $A\beta_{42}$ and sAPP β in brain at a magnitude similar to that of $A\beta_{40}$ (not shown). One representative compound from Table 1 is (S)-10, and the dose- and time-dependent reduction of $A\beta_{40}$ in brain is shown in Figure 4. The maximum reduction (50%) was seen 1.5 h after a 300 μ mol/kg dose of (S)-10. The free plasma and brain concentrations (C_u (plasma) and C_u (brain), respectively)³⁴ 1.5 h after dosing are summarized in Table 4. Pharmacokinetic/pharmacodynamic (PK/PD) modeling of (S)-10 time- and dose-response effect data in vivo, using an indirect response model with inhibition on the $A\beta$ production rate, estimated the unbound brain concentration giving 20% inhibition from baseline to 114 nM for (S)-10. The fraction unbound (f_u) in brain was less than that in plasma, and the fraction unbound in brain was steeply correlated to lipophilicity (measured as $\log D$) in this series. The inhibition of $A\beta_{40}$ in mouse primary cortical neurons was determined (Table 4), and for compounds studied in the in vivo PD model, we found a good correlation between measured in vitro IC_{50} values and $A\beta_{40}$ reduction in the mouse brain.

For the compounds with methoxy or pyridone as the hydrogen bond acceptor (Table 2), a large variation of the in vivo efficacy was observed, mainly due to a larger variability in Caco-2 permeability, efflux, and brain fraction unbound values. One representative compound is (R)-19, and the dose- and time-dependent reduction of brain $A\beta_{40}$ levels is shown in Figure 5. The maximum reduction (40%) was seen 1.5 h after a 200 μ mol/kg dose of (R)-19. The free plasma and brain concentrations 1.5 h after dosing are summarized in Table 4.

Table 4. Fluoroaminoisindoles Reducing $A\beta_{40}$ in the Brain of C57BL/6 Mice

compd	BACE2 FRET K_i^a (nM)	IC_{50} (primary neurons) ^b (nM)	dose ^c (μ mol/kg)	$A\beta_{40}$ reduction at 1.5 h, %	C_u (plasma) (nM)	f_u (plasma) (%)	C_u (brain) (nM)	f_u (brain) (%)
(S)-25	790	68	300	61	4118	8.9	445	8.8
27	nd ^d	436	300	48	1221	4.1	883	5.1
(S)-10	nd	204	300	50	795	4.4	406	2.5
(S)-32	370	51	80	31	170	2.7	119	7.9
(S)-16	770	53	125	40	883	11	73	4.6
35	1700	40	75	50	237	9.6	13	1.1
37	740	30	300	32	16267	52	113	16
(R)-19	78	3.4	200	40	123	1.8	14	0.6
(R)-41	7.5	2.6	50	36	196	1.5	3	1.0

^a K_i values are the means of at least two experiments. ^b IC_{50} values are the means of at least two experiments. ^cOral administration. ^dnd = not determined.

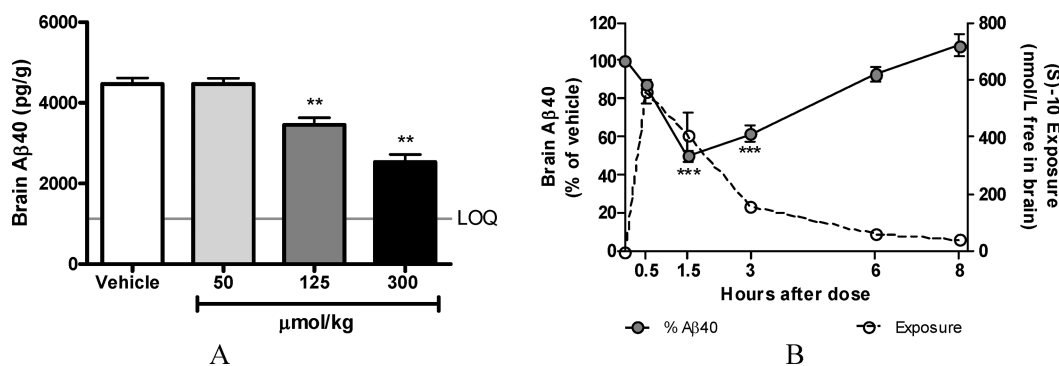


Figure 4. Reduction of Aβ40 levels in the brain of C57BL/6 mice after oral dosing of compound (S)-10. (A) Significant effects were seen 1.5 h after dosing with (S)-10 at 125 and 300 μmol/kg. (B) In the time–response study, significant effects were seen 1.5–3 h after dosing (300 μmol/kg). The free concentrations of (S)-10 were measured at different time points after dosing. Data are presented as mean values ± SEM (**, $P < 0.01$; ***, $P < 0.001$; compared to vehicle).

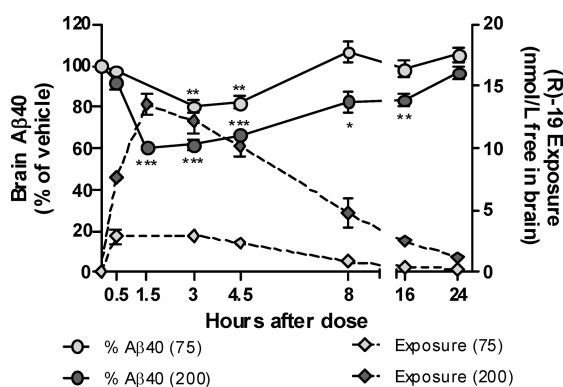


Figure 5. Reduction of Aβ40 levels in the brain of C57BL/6 mice after oral dosing of compound (R)-19, as shown in a dose- and time-response study (75 and 200 μmol/kg). At the higher dose (200 μmol/kg) significant reductions were seen 1.5–16 h after dosing, and significant effects were seen 3–4.5 h after the 75 μmol/kg dose. The free concentrations of (R)-19 in the brain were measured at different time points after dosing. Data are presented as mean values ± SEM (*, $P < 0.05$; **, $P < 0.01$; ***, $P < 0.001$; compared to vehicle).

(R)-19 demonstrated a very low fraction unbound (f_u) in brain and showed reduced access to the brain. The reduced brain access of (R)-19 could probably be explained by P-gp-induced efflux of the compound. The efflux ratio was later determined to be 5.1 in an MDCK-MDR1 cell-line assay. Even though this compound had a predicted low metabolic stability as evident from the intrinsic clearance (CL_{int}) value in rat hepatocytes and in vivo mouse PK analysis ($CL = 150$ mL/min/kg, po half-life 0.65 h), it still displayed a prolonged Aβ lowering effect in the in vivo PD experiments. Thus, compound (R)-19 displayed a better in vivo PD profile than would be expected from the in vitro and in vivo PK properties. PK/PD modeling of the time- and dose-response effect data in vivo estimated the unbound brain concentration giving 20% inhibition from baseline to 6 nM for (R)-19.

When comparing the results for different compounds in the in vivo PD experiments (Table 4) together with a combination of compound properties, it was evident that compound (S)-32 showed a superior profile. The concentration unbound brain/plasma ratio was determined to be 0.7, the highest in this compound series. The low lipophilicity of this compound was probably the explanation of why the fraction unbound in brain was higher than that in plasma for this compound. Compounds displaying large in vitro margins to hERG such as (S)-16 and

(R)-41 were found to have unfavorable unbound brain/plasma ratios, and thus, (S)-32 turned out to be the compound with the overall best properties for clinical evaluation.

CONCLUSION

In this paper we have disclosed an aminoisindole series as BACE1 inhibitors. Introducing a fluorine adjacent to the amidine moiety improved the permeability properties of the series and made it possible to achieve in vivo brain efficacy. Crystal structure information was used for structure-based design of new potent BACE1 inhibitors. Due to the basic nature of these compounds, they also displayed hERG affinity. Both lipophilicity and pK_a were used as means for reducing hERG inhibition, resulting in compound (S)-16 with an hERG IC_{50} value of 16 μM and BACE1 cell IC_{50} value of 8.6 nM. The BACE1 affinity of this series was further increased to subnanomolar levels, and compound (R)-41 with a cell IC_{50} value of 0.16 nM gave a high (>10000-fold) margin to the hERG IC_{50} . Several compounds were evaluated in vivo for reduction of the Aβ40 level in the brain of C57BL/6 mice. Compound (S)-32 showed a superior profile in the in vivo PD experiments with a concentration unbound brain/plasma ratio of 0.7. Despite the very good in vitro hERG margins, the in vivo margins to hERG side effects still remain a challenge for this series.

EXPERIMENTAL SECTION

hBACE1 and hBACE2 TR-FRET Assay. The soluble part of human β-secretase (recombinant hBACE1 enzyme, aa1–aa460, or hBACE2 enzyme, aa1–aa473) diluted in reaction buffer (sodium acetate, CHAPS, Triton X-100, EDTA, pH 4.5) was mixed with the test compound diluted in DMSO. After a preincubation period of 10 min, substrate, (europium)CEVNLDAEFK(Qsy7), was added and the reaction allowed to proceed for 15 min at room temperature (rt). The reaction was stopped by addition of 7 μL of sodium acetate, pH 9. The fluorescence of the product was measured on a Victor II plate reader with an excitation wavelength of 340 nm and an emission wavelength of 615 nm. The final concentration of the enzyme was 2.7 μg/mL (or 54 ng/mL); the final concentration of substrate was 100 nM. Reported values are means of $n \geq 2$ determinations, standard deviation $\leq 10\%$.

Cell sAPPβ Release Assay. SH-SY5Y cells (human neuroblastoma cell line) were cultured in DMEM/F-12 with Glutamax, 10% FCS, and 1% nonessential amino acids. The test compound was incubated with cells for 16 h at 37 °C, 5% CO₂. Meso Scale Discovery (MSD) plates were used for the detection of sAPPβ release; MSD sAPPβ plates were blocked in 3% BSA in Tris wash buffer for 1 h at rt and washed four times in Tris buffer. After incubation, 20 μL of medium was transferred

to the preblocked and washed 384-well MSD sAPP β microplate and incubated with shaking at rt for 2 h followed by washing four times in Tris buffer. A 10 μ L volume of detection antibody was added (1 nM) followed by incubation with shaking at rt for 2 h followed by washing four times in Tris buffer. A 40 μ L volume of read buffer was added per well, and the plates were read in a SECTOR imager. In addition, the cells incubated with test compound were further lysed and analyzed for any cytotoxic effects of the compounds using the ViaLight Plus cell proliferation/cytotoxicity kit (Cambrex BioScience) according to the manufacturer's instructions. Reported values are means of $n \geq 2$ determinations, standard deviation $\leq 10\%$.

Mouse Primary Neuron A β 40 Release Assay. Primary cortical cells were isolated from fetal C57/BL6 mice (E16). The cortices were kept in calcium- and magnesium-free Earle's balanced salt solution (CMF-EBSS) containing 0.25% trypsin and 2 U/mL DNase for 1 h at 37 $^{\circ}$ C and 5% CO₂. The cortices were washed in warm CMF-EBSS and gently triturated with flame-polished pipets to separate the cells. The cell solution was transferred to a 50 mL Falcon tube containing medium (10% HamsF12, 10% fetal bovine serum, 1% 10 mM HEPES, 1% 2 mM L-glutamine, 0.5% 50 U/0.5 mg penicillin-streptomycin, and 77.5% DMEM with 4.5 g/L glucose) and filtered through a 100 μ m cell strainer (BD Falcon). The cells were counted and plated onto 96-well poly-D-lysine-coated plates at a density of 200 000 cells/200 μ L/well. After five DIV at 37 $^{\circ}$ C and 5% CO₂, the medium was exchanged to medium containing the compounds at a final concentration of 1% DMSO and incubated overnight. The amount of released A β 40 in the extracellular medium was measured using Invitrogen Biosource enzyme-linked immunosorbent assay (ELISA) strips (KMB3481) according to the manufacturer's instructions. The strips were read using a Spektramax microplate reader (Molecular Devices). The cytotoxic effect of the compounds was directly evaluated on the cell plates utilizing a commercial cell proliferation/cytotoxicity kit based on luciferase reaction on ATP released by cells.

Protein Crystallography. The BACE1 protein used for structure determination was expressed and purified as previously described by Patel et al.³² and crystallized according to Swahn et al.¹⁶ Crystallographic data of BACE1 in complex with **10** were collected at 100 K on a Rigaku FR-E generator equipped with a Rigaku HTC detector to 1.79 \AA resolution and processed with MOSFLM³⁵ and SCALA.³⁶ For the (R)-**41** soaked crystal, data were collected at 100 K to 1.83 \AA on a Rigaku FR-E+ generator with a Rigaku Saturn A200 charge-coupled device (CCD) detector and processed with autoPROC³⁷ from Global Phasing utilizing XDS³⁸ and SCALA.³⁶ The crystals belong to space group P2₁2₁2₁, with one complex per asymmetric unit. A total of 5% of the reflections were used to calculate R_{free}. The structures were solved by rigid body refinement using Refmac5³⁹ and a previously determined BACE1 structure based on the published 1FKN structure.²¹ The ligands were well-defined in the difference electron density. Refmac5³⁹ and AUTOBUSTER⁴⁰ were used for crystallographic refinement, and Coot⁴¹ was used for model building. Data collection and refinement statistics are listed in Table 3. The coordinates for the crystal structures of **10** and (R)-**41** with BACE1 have been deposited with the RCSB Protein Data Bank. All figures showing structural representations were prepared using PyMOL.⁴²

Permeability Assay. Caco-2 cells were grown for 14–21 days to achieve confluency and polarization before being used for transport experiments. For both apical to basolateral (A–B) and basolateral to apical (B–A) transport directions, the pH was adjusted to 7.4. All compounds were investigated at a concentration of 10 μ M. Buffer volumes in the 24-well plates were 0.20 mL on the apical side and 0.80 mL on the basolateral side. Samples were withdrawn after 60 min from both sides. The integrity of the epithelial cell monolayer was monitored by measuring the passive transmembrane diffusion of [¹⁴C]mannitol. Concentrations of compounds in donor and receiver samples were analyzed by liquid chromatography–tandem mass spectrometry. Liquid scintillation was used for analysis of [¹⁴C]mannitol. The apparent permeability coefficient (P_{app}) was calculated according to $P_{app} = (dQ/dt)/(A C_0)$, where dQ/dt is the slope at 60 min of the graph of the cumulative amount transported vs time, A is

the surface area of the membrane, and C_0 is the starting concentration. The efflux ratio is the ratio $P_{app}(B-A)/P_{app}(A-B)$.

In Vivo Pharmacodynamic Assay. Female C57BL/6 mice (Harlan, The Netherlands), 8–14 weeks of age ($n = 6$ –12 per group) received vehicle (0.3 M gluconic acid) or BACE1 inhibitor as a single dose (50–300 μ mol/kg) via oral gavage. Animals were anaesthetized 0.5–24 h after administration, and blood was collected by heart puncture into prechilled microtainer tubes containing EDTA. Plasma samples were prepared by centrifugation for 10 min at approximately 3000g at 4 $^{\circ}$ C, and the samples were then stored at -70 $^{\circ}$ C until exposure and A β 40 analysis. After blood sampling, the animals were sacrificed by decapitation, and the brains were dissected out, the cerebellum and olfactory bulbs were removed, and the cerebrum was divided into left and right hemispheres. Both hemispheres were weighed, snap-frozen, and stored at -70 $^{\circ}$ C until exposure and A β 40 analysis, respectively. Prior to analysis, the left hemispheres were homogenized in 0.2% diethylamine (DEA) with 50 mM NaCl, followed by ultracentrifugation. Recovered supernatants were neutralized to pH 8.0 with 2 M Tris–HCl, snap-frozen on dry ice, and stored at -70 $^{\circ}$ C. A β 40 levels in brain extracts and plasma were analyzed using a highly specific commercial A β _{1–40} ELISA (KMB3481, Invitrogen, Camarillo, CA). Drug concentrations in brain (right hemisphere) and plasma samples were determined by reversed-phase liquid chromatography and electrospray tandem mass spectrometry. Analysis of A β data was performed using Prism 4 (GraphPad, La Jolla, CA), with one-way analysis of variance (ANOVA) followed by Dunnett's multiple comparison test or Bonferroni's multiple comparison test. The level of significance was set at $P < 0.05$.

Chemistry. All solvents used were commercially available and were used without further purification. Reactions were typically run using anhydrous solvents under an inert atmosphere of nitrogen or argon. Starting materials used were available from commercial sources or prepared as described in the Supporting Information. Room temperature refers to 20–25 $^{\circ}$ C. Microwave heating was performed in a Biotage Initiator microwave synthesizer at the indicated temperature in the recommended microwave tubes.

¹H NMR spectra were recorded in the indicated deuterated solvent at 400 MHz, and the spectra were obtained unless stated otherwise using a Bruker av400 NMR spectrometer equipped with a 3 mm flow injection SEI ¹H/D–¹³C probe head with Z-gradients using a BEST 215 liquid handler for sample injection or using a Bruker DPX400 NMR spectrometer equipped with a four-nucleus probehead (¹⁹F) with Z-gradients. Spectra (500 MHz) were recorded using a Bruker 500 MHz Avance III NMR spectrometer. Chemical shifts are given in parts per million down- and upfield from TMS. Resonance multiplicities are denoted s, d, t, q, m, and br for singlet, doublet, triplet, quartet, multiplet, and broad, respectively.

Preparative HPLC was performed on a Waters Auto purification HPLC–UV system with a diode array detector using a Waters XTerra MS C₈ column (19 \times 300 mm, 7 μ m), and a linear gradient of mobile phase B was applied. Mobile phase A was 0.1 M ammonium acetate in water/acetonitrile (95:5), and mobile phase B was acetonitrile. The flow rate was 20 mL/min. Flash chromatography was performed using Merck silica gel 60 (0.040–0.063 mm) or employing a Combi Flash Companion system using RediSep normal-phase flash columns.

LC–MS analyses were performed on an LC–MS system consisting of a Waters sample manager 2777C, a Waters 1525 μ binary pump, a Waters 1500 column oven, a Waters ZQ single-quadrupole mass spectrometer, a Waters PDA 2996 diode array detector, and a Sedex 85 ELS detector. The mass spectrometer was equipped with an electrospray (ES) ion source operated in positive and negative ion modes. For separation a linear gradient was applied starting at 100% (0.1% NH₃ in Milli-Q water) and ending at 100% methanol. The column used was an XBridge C18, 3.0 \times 50 mm, 5 μ m, which was run at a flow rate of 2 mL/min. Alternatively, an LC–MS system consisting of a Waters Alliance 2795 HPLC instrument, a Waters PDA 2996 diode array detector, a Sedex 85 ELS detector, and a ZQ single-quadrupole mass spectrometer was used. The mass spectrometer was equipped with an ES ion source operated in positive and negative ion modes. Separation was performed on an XBridge C18 column, 3.0 \times

50 mm, 3.5 μ m, run at a flow rate of 1 mL/min. A linear gradient was applied starting at 100% (0.1% NH₃ in Milli-Q water) and ending at 100% methanol.

Purity analyses were performed on an Agilent HP1100 system consisting of a G1322A Micro vacuum degasser, a G1312A binary pump, a G1367A well-plate autosampler, a G1316A thermostated column compartment, a G1315C diode array detector, and a 6120, G1978B mass spectrometer. The mass spectrometer was configured with an atmospheric pressure chemical ionization (APCI) ion source operated in positive and negative ion modes. The column used was an XBridge C18, 3.0 \times 100, 3 μ m, run at a flow rate of 1.0 mL/min. A linear gradient was used for both the blank and the sample, starting at 100% 10 mM NH₄OAc in 5% CH₃CN and ending at 95% CH₃CN. The blank run was subtracted from the sample run. All tested compounds were purified to >95% purity as determined by reversed-phase HPLC.

SFC purity analysis was run on an SFC Berger Analytix system with an Agilent 1100 photodiode array (PDA) detector. The column was a Chiralpak AD-H, 5 μ m, 4.6 \times 250 mm. The column temperature was set to 50 °C. An isocratic condition of 20–30% (methanol + 0.1% DEA) and 70–80% CO₂ was applied at a flow rate of 3.0 mL/min. The PDA was scanned from 190 to 600 nm, and 220 nm was extracted for purity determination. All tested compounds were purified to >99% enantiomeric purity as determined by SFC.

SFC preparative chromatography was run on an SFC Berger Multigram II system with a Knauer K-2501 UV detector. The column was a Chiralpak AD-H, 5 μ m, 21.2 \times 250 mm. The column temperature was set to 35 °C. An isocratic condition of 20–30% (methanol + 0.1% DEA) and 70–80% CO₂ was applied at a flow rate of 50.0 mL/min. The UV detector scanned at 220 nm. The UV signal determined the fraction collection.

2-(3-Bromo-4-fluorobenzoyl)-6-fluorobenzonitrile (7). To a solution of (2-cyano-3-fluorophenyl)zinc(II) iodide (80.0 mL, 40.0 mmol, 0.5 M in THF) was added tetrakis(triphenylphosphine)-palladium(0) (2.3 g, 2.0 mmol) in small portions at 0 °C. A solution of 3-bromo-4-fluorobenzoyl chloride (10.0 g, 42.1 mmol) in anhydrous THF (20 mL) was then added dropwise, and the reaction mixture was stirred at 0 °C for 1 h. The reaction was quenched by addition of water (150 mL), and the resulting mixture was extracted with ethyl acetate (2 \times 150 mL). The combined organic extracts were washed with brine, dried over sodium sulfate, and concentrated in vacuo. The product was purified by flash chromatography to afford the title compound (7.90 g, 61% yield): ¹H NMR (500 MHz, DMSO-*d*₆) δ (ppm) 7.58–7.64 (m, 2 H) 7.83 (t, *J* = 8.91 Hz, 1 H) 7.88 (ddd, *J* = 8.55, 4.77, 2.13 Hz, 1 H) 7.93 (td, *J* = 8.12, 5.67 Hz, 1 H) 8.14 (dd, *J* = 6.70, 2.13 Hz, 1 H); ¹⁹F NMR (400 MHz, CDCl₃) δ (ppm) –97.16, –103.63; MS (ESI, positive ion) *m/z* 322, 324 (*M* + 1).

***N*-(3-Bromo-4-fluorophenyl)(2-cyano-3-fluorophenyl)methylene)-2-methylpropane-2-sulfonamide (8).** 2-(3-Bromo-4-fluorobenzoyl)-6-fluorobenzonitrile (7.9 g, 24.5 mmol) dissolved in dry THF (40 mL) was added to a solution of titanium(IV) ethoxide (12.7 mL, 61.3 mmol) in dry THF (30 mL) at rt. 2-Methyl-2-propanesulfonamide (3.57 g, 29.4 mmol) was added, and the resulting mixture was heated at reflux temperature for 22 h. The reaction mixture was cooled to rt, and then methanol (120 mL) was added, followed by addition of saturated aqueous Na₂CO₃ (12 mL). The resulting suspension was filtered through a pad of sodium sulfate, and the solids were washed thoroughly with ethyl acetate. The filtrate was concentrated in vacuo and purified by flash chromatography to afford the title compound (5.7 g, 55% yield): ¹H NMR (400 MHz, CDCl₃) δ (ppm) 1.37 (s, 9 H), 7.19 (t, *J* = 8.2 Hz, 1 H), 7.22 (m, 1 H), 7.36–7.32 (m, 1 H), 7.48 (m, 1 H), 7.72–7.67 (m, 1 H), 7.81 (m, 1 H); ¹⁹F NMR (400 MHz, CDCl₃) δ (ppm) –99.65, –100.18, –104.55, –105.17; MS (ESI, positive ion) *m/z* 424, 426 (*M* + 1).

1-(3-Bromo-4-fluorophenyl)-4-fluoro-1-(2-(trifluoromethyl)pyridin-4-yl)-1*H*-isoindol-3-amine (9). *tert*-Butyllithium (1.6 M in pentane) (6.08 mL, 9.73 mmol) was slowly added to dry THF (40 mL) at –100 °C under an argon atmosphere. 4-Bromo-2-(trifluoromethyl)pyridine (1.1 g, 4.87 mmol) in dry THF (8.0 mL) was added dropwise. After 10 min *N*-((3-bromo-4-fluorophenyl)(2-

cyano-3-fluorophenyl)methylene)-2-methylpropane-2-sulfonamide (2.07 g, 4.87 mmol) in dry THF (8.0 mL) was added dropwise, and the resulting reaction mixture was stirred at –100 °C for 30 min and then allowed to reach rt. The reaction was quenched by addition of water and extracted with ethyl acetate (3 \times). The combined organic extracts were washed (brine), dried (Na₂SO₄), and concentrated in vacuo. The residue was dissolved in methanol (40 mL), and hydrochloric acid (2.0 M in diethyl ether) (7.3 mL, 14.6 mmol) was added. The mixture was stirred at rt overnight and subsequently concentrated in vacuo. The residue was partitioned between saturated aqueous Na₂CO₃ and dichloromethane (3 \times), and the combined organic layers were dried (Na₂SO₄), filtered, and concentrated in vacuo. Purification by flash chromatography gave the title compound (1.14 g, 50% yield): ¹H NMR (500 MHz, DMSO-*d*₆) δ (ppm) 6.86 (br s, 1 H), 7.27–7.42 (m, 3 H), 7.53–7.63 (m, 2 H), 7.64 (ddd, *J* = 5.24, 0.91, 0.79 Hz, 1 H), 7.67 (d, *J* = 0.79 Hz, 1 H), 7.76 (d, *J* = 7.57 Hz, 1 H), 8.70 (d, *J* = 5.52 Hz, 1 H); MS (ESI, positive ion) *m/z* 468, 470 (*M* + 1).

4-Fluoro-1-(4-fluoro-3-(pyrimidin-5-yl)phenyl)-1-(2-(trifluoromethyl)pyridin-4-yl)-1*H*-isoindol-3-amine (10). 1-(3-Bromo-4-fluorophenyl)-4-fluoro-1-(2-(trifluoromethyl)pyridin-4-yl)-1*H*-isoindol-3-amine (0.30 g, 0.64 mmol) and 5-pyrimidinylboronic acid (0.104 g, 0.84 mmol) in DMF (5.0 mL) were heated to 90 °C under an argon atmosphere. Pd^{II}Cl₂dppf·CH₂Cl₂ (0.039 g, 0.05 mmol) and aqueous K₂CO₃ (2.0 M) (0.96 mL, 1.92 mmol) were added, and the resulting mixture was stirred at 90 °C for 1 h. The reaction mixture was cooled to rt and then purified by preparative HPLC to give the title compound (0.16 g, 51% yield): ¹H NMR (500 MHz, DMSO-*d*₆) δ (ppm) 6.83 (br s, 2 H), 7.31 (dd, *J* = 9.38, 8.43 Hz, 1 H), 7.37 (dd, *J* = 10.25, 8.83 Hz, 1 H), 7.51 (ddd, *J* = 8.67, 4.89, 2.36 Hz, 1 H), 7.54–7.62 (m, 2 H), 7.68 (dd, *J* = 5.04, 1.42 Hz, 1 H), 7.71 (d, *J* = 0.95 Hz, 1 H), 7.86 (d, *J* = 7.57 Hz, 1 H), 8.70 (d, *J* = 5.20 Hz, 1 H), 8.95 (d, *J* = 1.26 Hz, 2 H), 9.21 (s, 1 H); MS (ESI, positive ion) *m/z* 468 (*M* + 1).

(*S*)-4-Fluoro-1-(4-fluoro-3-(pyrimidin-5-yl)phenyl)-1-(2-(trifluoromethyl)pyridin-4-yl)-1*H*-isoindol-3-amine ((*S*)-10). 4-Fluoro-1-(4-fluoro-3-(pyrimidin-5-yl)phenyl)-1-(2-(trifluoromethyl)pyridin-4-yl)-1*H*-isoindol-3-amine (0.5 g, 1.1 mmol) was dissolved in methanol (20 mL), and the resulting solution was injected (20 stacked injections) on a Chiralpak AD column (21.2 \times 250 mm) using IPA (0.1% DEA)/CO₂ (20:80) as the eluent. The title compound was collected and concentrated in vacuo to yield 0.2 g, >99% enantiomerically pure: ¹H NMR (500 MHz, DMSO-*d*₆) δ (ppm) 6.83 (br s, 1 H), 7.32 (t, *J* = 8.83 Hz, 1 H), 7.37 (t, *J* = 9.46 Hz, 1 H), 7.48–7.54 (m, 1 H), 7.55–7.62 (m, 2 H), 7.68 (d, *J* = 5.20 Hz, 1 H), 7.71 (s, 1 H), 7.86 (d, *J* = 7.57 Hz, 1 H), 8.70 (d, *J* = 5.04 Hz, 1 H), 8.95 (dd, *J* = 0.95, 0.47 Hz, 2 H), 9.21 (s, 1 H); MS (ESI, positive ion) *m/z* 468 (*M* + 1).

2-((2-Difluoromethyl)pyridin-4-yl)carbonyl)-4,6-difluorobenzonitrile (13). LiCl (244 mg, 5.75 mmol) was added to a solution of 2-(difluoromethyl)isonicotinic acid (1.0 g, 5.77 mmol) in anhydrous acetonitrile (30 mL), and the mixture was stirred at 55 °C for 30 min. The mixture was cooled to rt, and DMF (0.09 mL, 1.16 mmol) was added followed by dropwise addition of oxalyl chloride (0.54 mL, 6.29 mmol). The mixture was stirred for 1 h at rt and then concentrated slowly over 1 h at 45 °C to a 10 mL volume. The mixture was cooled to rt, and CuCN (103 mg, 1.15 mmol) and (2-cyano-3,5-difluorophenyl)zinc bromide (0.1 M in THF) (69 mL, 6.9 mmol) were added. The mixture was stirred at rt for 2 h and then concentrated in vacuo. The residue was treated with 10% L-ascorbic acid, and the aqueous phase was extracted with DCM and with EtOAc. The combined extracts were washed with sodium phosphate monobasic (10% solution), dried over MgSO₄, and concentrated. The residue was purified by flash chromatography to give the title compound (310 mg, 18% yield): ¹H NMR (400 MHz, CDCl₃) δ (ppm) 6.74 (t, *J*_{HF} = 56 Hz, 1H), 7.18–7.22 (m, 1 H), 7.27–7.31 (m, 1 H), 7.74 (d, *J* = 5.08 Hz, 1 H), 7.92 (s, 1 H), 8.94 (d, *J* = 5.08 Hz, 1 H); MS (ESI, positive ion) *m/z* 295 (*M* + 1).

***N*-((2-Cyano-3,5-difluorophenyl)(2-(difluoromethyl)-4-pyridyl)methylene)-2-methylpropane-2-sulfonamide (14).** Ti(OEt)₄ (0.54 mL, 2.57 mmol) and 2-methylpropane-2-sulfonamide (198 mg, 1.62 mmol) were added to a stirred solution of 2-((2-

(difluoromethyl)pyridin-4-yl)carbonyl)-4,6-difluorobenzonitrile (300 mg, 1.01 mmol) in dry THF (30 mL). The reaction mixture was heated at 60 °C for 36 h and then cooled to rt. MeOH (2 mL) and saturated aqueous NaHCO₃ (0.5 mL) were added. The mixture was stirred for 2 h at rt and then filtered through a pad of Celite and MgSO₄. The solids were washed with THF (60 mL), and the filtrate was concentrated in vacuo. The residue was purified by flash chromatography to give the title compound (260 mg, 64% yield): ¹H NMR (400 MHz, CDCl₃) δ (ppm) 1.43 (s, 9 H), 6.79 (t, *J*_{HF} = 56 Hz, 1H), 6.74–6.80 (m, 1 H), 6.94 (dd, *J* = 8.99, 1.95 Hz, 1 H), 7.56 (d, *J* = 4.30 Hz, 1 H), 7.79 (s, 1 H), 8.67 (d, *J* = 5.47 Hz, 1 H); MS (ESI, positive ion) *m/z* 398 (M + 1).

3-(3-Bromophenyl)-3-(2-(difluoromethyl)pyridin-4-yl)-5,7-difluoro-3H-isoindol-1-amine (15). *n*-BuLi (0.5 mL, 1.25 mmol) was added to a solution of 1,3-dibromobenzene (243 mg, 1.03 mmol) in dry THF (50 mL) at –78 °C. The mixture was stirred for 30 min and then added to a solution of *N*-((2-cyano-3,5-difluorophenyl)(2-(difluoromethyl)-4-pyridyl)methylene)-2-methylpropane-2-sulfinamide (205 mg, 0.51 mmol) in THF (5 mL) at –78 °C. The mixture was stirred at –78 °C for 15 min and then at 0 °C for 30 min. The reaction was quenched by addition of methanolic HCl (1.25 M, 6 mL), neutralized using saturated aqueous NaHCO₃ solution, and extracted with EtOAc. The combined organic extracts were dried over MgSO₄ and concentrated in vacuo. The residue was purified by flash chromatography to afford the title compound (180 mg, 78% yield): ¹H NMR (400 MHz, CDCl₃) δ (ppm) 6.79 (t, *J*_{HF} = 56 Hz, 1H), 6.92 (td, *J* = 9.09, 1.76 Hz, 1 H), 7.06 (dd, *J* = 7.42, 1.95 Hz, 1 H), 7.16 (s, 1 H), 7.17–7.22 (m, 1 H), 7.32 (d, *J* = 5.08 Hz, 1 H), 7.39 (d, *J* = 1.95 Hz, 1 H), 7.44 (d, *J* = 7.82 Hz, 1 H), 7.52 (s, 1 H), 8.58 (d, *J* = 5.47 Hz, 1 H); MS (ESI, positive ion) *m/z* 450, 452 (M + 1).

1-[2-(Difluoromethyl)pyridin-4-yl]-4,6-difluoro-1-(3-pyrimidin-5-ylphenyl)-1H-isoindol-3-amine (16). K₂CO₃ (83 mg, 0.60 mmol) and pyrimidin-5-ylboronic acid (37 mg, 0.29 mmol) were added to a solution of 3-(3-bromophenyl)-3-(2-(difluoromethyl)pyridin-4-yl)-5,7-difluoro-3H-isoindol-1-ylamine (90 mg, 0.20 mmol) in a DME/EtOH/H₂O mixture (3:2:1, 12 mL). The mixture was degassed for 30 min, and then PdCl₂(PPh₃)₂ (14 mg, 0.02 mmol) was added. The reaction mixture was heated at 100 °C for 3 h, cooled to room temperature, filtered, and concentrated in vacuo. The residue was purified by flash chromatography to give the title compound (24 mg, 26% yield): ¹H NMR (400 MHz, CDCl₃) δ (ppm) 6.76 (t, *J*_{HF} = 56 Hz, 1H), 7.08 (t, *J* = 8.79 Hz, 1 H), 7.16 (dd, *J* = 7.23, 1.76 Hz, 1 H), 7.31 (d, *J* = 8.21 Hz, 1 H), 7.41 (d, *J* = 4.69 Hz, 1 H), 7.49 (s, 1 H), 7.52–7.57 (m, 2 H), 7.58–7.63 (m, 1 H), 8.67 (d, *J* = 5.08 Hz, 1 H), 8.92 (s, 2 H), 9.22 (s, 1 H); ¹⁹F NMR (376 MHz, CDCl₃) δ (ppm) –76.4, –116.2; MS (ESI, positive ion) *m/z* 450 (M + 1).

(S)-1-[2-(Difluoromethyl)pyridin-4-yl]-4,6-difluoro-1-(3-pyrimidin-5-ylphenyl)-1H-isoindol-3-amine ((S)-16). 1-[2-(Difluoromethyl)pyridin-4-yl]-4,6-difluoro-1-(3-pyrimidin-5-ylphenyl)-1H-isoindol-3-amine was subjected to enantiomer separation using SFC preparative chromatography to yield the title compound with an enantiomeric purity of 99.7%: ¹H NMR (400 MHz, CDCl₃) δ (ppm) 6.76 (t, *J*_{HF} = 56 Hz, 1H), 7.08 (t, *J* = 8.79 Hz, 1 H), 7.16 (dd, *J* = 7.23, 1.76 Hz, 1 H), 7.31 (d, *J* = 8.21 Hz, 1 H), 7.41 (d, *J* = 4.69 Hz, 1 H), 7.49 (s, 1 H), 7.52–7.57 (m, 2 H), 7.58–7.63 (m, 1 H), 8.67 (d, *J* = 5.08 Hz, 1 H), 8.92 (s, 2 H), 9.22 (s, 1 H); ¹⁹F NMR (376 MHz, CDCl₃) δ (ppm) –76.4, –116.2; MS (ESI, positive ion) *m/z* 450 (M + 1).

2-(3-Bromobenzoyl)-6-fluorobenzonitrile (17a). A solution of copper(I) cyanide (4.7 g, 52.5 mmol) and lithium bromide (2.63 mL, 105.0 mmol) in THF (65 mL) was added to (2-cyano-3-fluorophenyl)zinc(II) iodide (100 mL, 50 mmol) at –78 °C under an argon atmosphere. The mixture was stirred at rt for 1 h and then cooled to –78 °C. 3-Bromobenzoyl chloride (6.94 mL, 52.5 mmol) was added dropwise, and the mixture was stirred at rt for 4 h. Then aqueous NH₄Cl (50 mL) was added followed by water (50 mL). The THF was removed in vacuo, and the aqueous residue was diluted with water (100 mL) and DCM (150 mL). A precipitate was filtered off, and the filtrate was added to a separation funnel. The organic layer was separated and the water phase extracted with DCM (100 mL). The

combined organics were washed with brine (150 mL), dried over MgSO₄, concentrated, and purified with flash chromatography to give the title compound (13.4 g, 88% yield): ¹H NMR (600 MHz, DMSO-*d*₆) δ (ppm) 7.56 (t, *J* = 8.11 Hz, 1 H), 7.60–7.65 (m, 1 H), 7.77–7.86 (m, 2 H), 7.90–7.94 (m, 1 H), 7.95–7.99 (m, 2 H); MS (ESI, positive ion) *m/z* 304, 306 (M + 1).

***N*-((3-Bromophenyl)(2-cyano-3-fluorophenyl)methylene)-2-methylpropane-2-sulfinamide (17).** Titanium ethoxide (7.13 mL, 34.6 mmol), 2-methyl-2-propanesulfinamide (2.73 g, 22.5 mmol), and 2-(3-bromobenzoyl)-6-fluorobenzonitrile (5.26 g, 17.3 mmol) in dry THF (57 mL) were refluxed overnight under an argon atmosphere. The solution was allowed to cool to rt and was then transferred to an open flask containing MeOH (150 mL), aqueous NaHCO₃ (30 mL), and EtOAc (600 mL). The resulting mixture was stirred for 25 min and was then filtered through a mixture of Celite and Na₂SO₄ and concentrated. The product was purified by flash chromatography to give the title compound (5.96 g, 85% yield): ¹H NMR (500 MHz, DMSO-*d*₆) δ (ppm) 1.28 (br s, 9 H), 7.44–7.55 (m, 3 H), 7.67 (m, 1 H), 7.71–7.76 (m, 1 H), 7.81–7.97 (m, 2 H); MS (ESI, positive ion) *m/z* 407, 409 (M + 1).

(S)-*N*-((3-Bromophenyl)(2-cyano-3-fluorophenyl)methylene)-2-methylpropane-2-sulfinamide ((S)-17). Following the procedure described for 17 using commercially available (S)-2-methyl-2-propanesulfinamide gave the corresponding enantiomerically pure (S)-*N*-((3-bromophenyl)(2-cyano-3-fluorophenyl)methylene)-2-methylpropane-2-sulfinamide.

(S)-*N*-((2-Cyano-3-fluorophenyl)(3-(cyclopropylethynyl)phenyl)methylene)-2-methylpropane-2-sulfinamide ((S)-18). (S)-*N*-((3-Bromophenyl)(2-cyano-3-fluorophenyl)methylene)-2-methylpropane-2-sulfinamide (27.7 g, 68.1 mmol), bis-(triphenylphosphine)palladium(II) chloride (2.39 g, 3.4 mmol), and copper(I) iodide (1.3 g, 6.8 mmol) were dissolved in dry 2-methyltetrahydrofuran (70 mL) at rt under a nitrogen atmosphere. Ethynylcyclopropane (11.5 mL, 136 mmol) and triethylamine (33 mL, 238 mmol) were added, and the resulting mixture was stirred at 60 °C overnight. Additional copper(I) iodide (1.3 g, 6.8 mmol), bis-(triphenylphosphine)palladium(II) chloride (1.4 g, 2.0 mmol), and ethynylcyclopropane (5.7 mL, 68.0 mmol) were added, and the mixture was heated at 60 °C for 6 h. After the mixture was cooled to rt, ethyl acetate was added followed by water and saturated aqueous NaHCO₃. The organic layer was collected, activated charcoal was added, and the mixture was stirred for 3 min, after which it was filtered through Celite and concentrated. Purification by flash chromatography gave the title compound (22.6 g, 84% yield): ¹H NMR (500 MHz, DMSO-*d*₆) δ (ppm) 0.74 (m, 2 H), 0.85–0.92 (m, 2 H), 1.27 (br s, 9 H), 1.54 (m, 1 H), 7.32–7.71 (m, 6 H), 7.88 (br s, 1 H); MS (ESI, positive ion) *m/z* 393 (M + 1).

(R)-5-(3-Amino-1-(3-(cyclopropylethynyl)phenyl)-4-fluoro-1H-isoindol-1-yl)-1-ethyl-3-methylpyridin-2(1H)-one ((R)-19). *n*-BuLi (2.5 M in hexanes) (1.76 mL, 4.4 mmol) was added to THF (3 mL) in a dry bottle at –40 °C (external temperature). Butylmagnesium chloride (2 M in THF) (1.03 mL, 2.05 mmol) was added dropwise over 3 min, and the resulting mixture was stirred for 30 min. Then 5-bromo-1-ethyl-3-methylpyridin-2(1H)-one (1.27 g, 5.8 mmol) in THF (5 mL) was added dropwise, and after 1 min, (S)-*N*-((2-cyano-3-fluorophenyl)(3-(cyclopropylethynyl)phenyl)methylene)-2-methylpropane-2-sulfinamide (1.15 g, 2.9 mmol) in THF (5 mL) was added. The mixture was allowed to reach rt and was then stirred for 1 h. EDTA (0.43 g, 1.5 mmol) in water (5 mL) was added followed by 6 M HCl (1.5 mL, 8.8 mmol). After the mixture was stirred for 10 min, aqueous NaHCO₃ was added, and the mixture was extracted with ethyl acetate. The organic phase was dried over MgSO₄, filtered, and concentrated. The residue was dissolved in THF (3 mL), and 1.25 M HCl in methanol (11.7 mL, 14.7 mmol) was added. After the mixture was stirred overnight, aqueous NaHCO₃ was added, and the mixture was extracted with ethyl acetate. The organic phase was dried over MgSO₄ and concentrated. Purification by flash chromatography gave the title compound (1.13 g, 91% yield) with a chiral purity of 70%. This material was subjected to enantiomer separation using SFC preparative chromatography to yield the title

compound with an enantiomeric purity of over 99.5%: ^1H NMR (500 MHz, DMSO- d_6) δ (ppm) 0.66–0.72 (m, 2 H), 0.81–0.88 (m, 2 H), 1.10–1.17 (m, 3 H), 1.46–1.54 (m, 1 H), 1.93 (s, 3 H), 3.76–3.89 (m, 2 H), 6.55 (br s, 2 H), 7.17–7.29 (m, 7 H), 7.51 (td, $J = 7.88$, 4.73 Hz, 1 H), 7.55–7.60 (m, 1 H); MS (ESI, positive ion) m/z 426 ($M + 1$).

(R)-5-(3-Amino-1-(3-bromophenyl)-4-fluoro-1H-isoindol-1-yl)-1-ethyl-3-methylpyridin-2(1H)-one ((R)-20). *n*-Butyllithium (53.4 mL, 133.4 mmol) and THF (100 mL) were added to a dry reactor. After the mixture was cooled to an inner temperature of -25 °C, *n*-butylmagnesium chloride (39.0 mL, 66.7 mmol) was added over 20 min. After 45 min, 5-bromo-1-ethyl-3-methylpyridin-2(1H)-one (39.9 g, 184.7 mmol) in THF (100 mL) was added over 30 min. After the mixture was stirred for an additional 30 min, (*S*)-*N*-((3-bromophenyl)(2-cyano-3-fluorophenyl)methylene)-2-methylpropane-2-sulfonamide (41.8 g, 102.6 mmol) dissolved in THF (100 mL) was added. The mixture was allowed to reach rt over 45 min, and then the mixture was stirred at rt for 2 h. After the mixture was cooled to -20 °C, EDTA (1.42 g) was added, followed by a mixture consisting of ammonium chloride (25.6 g) and water (150 mL). The mixture was allowed to reach rt over 50 min. After extractive workup with isopropyl acetate and DCM, the organic phases were dried (Mg_2SO_4), filtered, concentrated in vacuo to give the title compound with an enantiomeric purity of 73% (24 g, 53% yield). This material was subjected to enantiomer separation on a Chiralpak AD-H column (50 \times 300 mm) using 80% *n*-heptane/20% (EtOH + 0.1% DEA) as the eluent. The second eluting enantiomer was collected (11 g, 99.8% enantiomeric purity): ^1H NMR (600 MHz, DMSO- d_6) δ (ppm) 1.14 (t, $J = 7.12$ Hz, 3 H) 1.94 (s, 3 H) 3.83 (m, 2 H) 6.60 (br s, 2 H) 7.25 (m, 4 H) 7.33 (d, $J = 7.97$ Hz, 1 H) 7.42 (m, 2 H) 7.52 (td, $J = 7.79$, 4.77 Hz, 1 H) 7.60 (d, $J = 7.54$ Hz, 1 H); MS (ESI, positive ion) m/z 440, 442 ($M + 1$).

(R)-5-(3-Amino-1-(3-aminophenyl)-4-fluoro-1H-isoindol-1-yl)-1-ethyl-3-methylpyridin-2(1H)-one ((R)-21). A solution of (*R*)-5-(3-amino-1-(3-bromophenyl)-4-fluoro-1H-isoindol-1-yl)-1-ethyl-3-methylpyridin-2(1H)-one (1.0 g, 2.27 mmol), *trans*-4-hydroxy-L-proline (0.3 g, 2.27 mmol), copper(I) iodide (0.22 g, 1.14 mmol), and potassium carbonate (0.94 g, 6.8 mmol) was placed in a microwave vial. Dimethyl sulfoxide (8 mL) was added, and the mixture was stirred at rt for 1 h. Then ammonia (32% in H_2O) (3.5 mL, 66.1 mmol) was added via a syringe. The reaction mixture was heated at 110 °C for 3 h in a microwave reactor. The reaction mixture was diluted with brine and extracted with ethyl acetate. The organic phase was dried over MgSO_4 , filtered, and concentrated in vacuo. The product was purified by flash chromatography to give the title compound (176 mg, 21%): ^1H NMR (500 MHz, DMSO- d_6) δ (ppm) 1.05–1.18 (m, 4 H), 1.94 (s, 3 H), 3.17 (d, $J = 5.04$ Hz, 2 H), 5.01 (br s, 2 H), 6.23–6.67 (m, 5 H), 6.89 (t, $J = 7.72$ Hz, 1 H), 7.15–7.30 (m, 3 H), 7.44–7.55 (m, 2 H); MS (ESI, positive ion) m/z 377 ($M + 1$).

(R)-N-(3-(3-Amino-1-(1-ethyl-5-methyl-6-oxo-1,6-dihydro-pyridin-3-yl)-4-fluoro-1H-isoindol-1-yl)phenyl)-5-chloropicolinamide ((R)-22). 5-Chloropicolinic acid (0.047 g, 0.30 mmol) and 1-(3-(dimethylamino)propyl)-3-ethylcarbodiimide hydrochloride (0.06 g, 0.32 mmol) were added to a dry vial. DCM (2 mL) was added, and the mixture was stirred for 5 min. The reaction mixture was then added dropwise to a cold (0 °C) solution of (*R*)-5-(3-amino-1-(3-aminophenyl)-4-fluoro-1H-isoindol-1-yl)-1-ethyl-3-methylpyridin-2(1H)-one (0.09 g, 0.23 mmol) in *N,N*-dimethylformamide (2 mL) and hydrochloric acid (3 M) (0.07 mL, 0.21 mmol). The reaction mixture was stirred at 0 °C for 1 h, then allowed to reach rt, and stirred overnight. The reaction was quenched by addition of MeOH (1 mL), and stirring was continued for 1 h. The reaction mixture was partitioned between saturated aqueous Na_2CO_3 solution and ethyl acetate, and the organic phase was dried over MgSO_4 , filtered, and concentrated in vacuo. Purification performed by preparative HPLC gave the title compound (0.07 g, 57% yield): ^1H NMR (500 MHz, DMSO- d_6) δ (ppm) 1.08–1.20 (m, 3 H), 1.94 (s, 3 H), 3.84 (q, $J = 7.25$ Hz, 2 H), 6.52 (br s, 2 H), 7.05 (d, $J = 7.88$ Hz, 1 H), 7.21–7.29 (m, 5 H), 7.51 (td, $J = 7.80$, 4.89 Hz, 1 H), 7.55–7.60 (m, 1 H), 7.79

(d, $J = 7.88$ Hz, 1 H), 7.82 (s, 1 H), 8.10–8.15 (m, 1 H), 8.16–8.22 (m, 1 H), 8.75 (d, $J = 2.21$ Hz, 1 H), 10.62 (s, 1 H); MS (ESI, positive ion) m/z 516 ($M + 1$).

(R)-5-(3-Amino-4-fluoro-1-(3-(5-prop-1-ynylpyridin-3-yl)phenyl)-1H-isoindol-1-yl)-1-ethyl-3-methylpyridin-2(1H)-one ((R)-41). (*R*)-20 (143 mg, 0.32 mmol), (5-prop-1-ynylpyridin-3-yl)boronic acid (105 mg, 0.65 mmol), $\text{Pd}^{\text{II}}\text{Cl}_2\text{dppf}\cdot\text{CH}_2\text{Cl}_2$ (13 mg, 0.02 mmol), 2 M aqueous K_2CO_3 (0.49 mL, 0.97 mmol), and dioxane (3 mL) were mixed in a vial and heated in a microwave reactor at 130 °C for 15 min. The mixture was concentrated, and the resulting residue was dissolved in DCM (3 mL) and water (2 mL). The organic phase was separated, concentrated, and purified by preparative HPLC to afford the title compound (91 mg, 59% yield, >99% enantiomerically pure): ^1H NMR (400 MHz, DMSO- d_6) δ (ppm) 1.14 (t, $J = 7.07$ Hz, 3 H), 1.93 (s, 3 H), 2.11 (s, 3 H), 3.76–3.91 (m, 2 H), 6.58 (br s, 2 H), 7.21–7.31 (m, 3 H), 7.39–7.46 (m, 2 H), 7.52 (td, $J = 7.89$, 4.93 Hz, 1 H), 7.56–7.63 (m, 2 H), 7.72 (d, $J = 7.58$ Hz, 1 H), 7.95 (t, $J = 2.02$ Hz, 1 H), 8.56 (d, $J = 1.77$ Hz, 1 H), 8.70 (d, $J = 2.27$ Hz, 1 H); MS (ESI, positive ion) m/z 477 ($M + 1$).

■ ASSOCIATED CONTENT

📄 Supporting Information

Synthetic procedures and analytical data for test compounds 23, 24, 25, (S)-25, 26, 27, 28, 29, 30, 31, 32, (S)-32, 33, 34, 35, 36, 37, 38, 39, 40, and (R)-42 and synthetic procedures for intermediates. This material is available free of charge via the Internet at <http://pubs.acs.org>.

Accession Codes

New protein/ligand coordinates for 10 and (R)-41 have been deposited in the PDB with IDs 4azy and 4b00, respectively.

■ AUTHOR INFORMATION

Corresponding Author

*Phone: +46 (0) 70 290 72 01. E-mail: brittmarieswahn@gmail.com.

Notes

The authors declare no competing financial interest.

■ ACKNOWLEDGMENTS

We specially thank NAEJA Pharmaceuticals Inc., Canada, for the supply of synthesized intermediates. We thank the Physicochemical Characterization Team at the Department of Medicinal Chemistry at AstraZeneca Södertälje for physicochemical characterization, the Analytical & Purification Sciences Team for enantiomer separations and purity determinations, and the Safety Assessment screening center at AstraZeneca Alderly Park for hERG assessments. We thank Martin Ekman and Martin Levin for FRET and sAPP β measurements and Ann-Cathrin Radesäter for measurements in primary neurons. We thank Carolina Sandman and Carrie Tsoi for Caco-2 measurements, Eva Floby and Anneli Bengtsson for rat hepatocyte CL_{int} values, Eva Spennare and Jenny Johansson for determination of the fraction unbound in brain and plasma protein binding, Stefan Martinsson, Jessie Dahlström, and Sveinn Briem for bioanalysis, Anna Aagaard for crystallization, and Madeleine Åhman for pK_a measurements. In addition, we thank the people involved in performing the in vivo experiments, Kristina Eliason, Daniel Bergström, Gunilla Ericsson, Anna Bogstedt, Ann Stafund, Anette Stålebring Löwstedt, Susanne Gustavsson, and Carina Stephan.

■ ABBREVIATIONS USED

BACE, β -site APP cleaving enzyme; AD, Alzheimer's disease; A β , β -amyloid; APP, amyloid- β precursor protein; sAPP β ,

soluble amyloid- β precursor protein; SAR, structure–activity relationship; PSA, polar surface area; ER, efflux ratio; PD, pharmacodynamic; C_w , concentration unbound; f_w , fraction unbound; DCM, dichloromethane; DEA, diethylamine; IPA, isopropyl alcohol; TEA, triethylamine; SFC, supercritical fluid chromatography; rt, room temperature

REFERENCES

- (1) Alzheimer's Association. Alzheimer's disease facts and figures. *Alzheimer's Dementia* **2010**, *6*, 158, 194.
- (2) Hardy, J.; Selkoe, D. J. The amyloid hypothesis of Alzheimer's disease: progress and problems on the road to therapeutics. *Science* **2002**, *297*, 353–356.
- (3) (a) Sinha, S.; Anderson, J. P.; Barbour, R.; Basi, G. S.; Caccavello, R.; Davis, D.; Doan, M.; Dovey, H. F.; Frigon, N.; Hong, J.; Jacobson-Croak, K.; Jewett, N.; Keim, P.; Knops, J.; Lieberburg, I.; Power, M.; Tan, H.; Tatsuno, G.; Tung, J.; Schenk, D.; Seubert, P.; Suomensari, S. M.; Wang, S.; Walker, D.; Zhao, J.; McConlogue, L.; John, V. Purification and cloning of amyloid precursor protein β -secretase from human brain. *Nature* **1999**, *402*, 537–540. (b) Vassar, R.; Bennett, B. D.; Babu-Khan, S.; Kahn, S.; Mendiaz, E. A.; Denis, P.; Teplow, D. B.; Ross, S.; Amarante, P.; Loeloff, R.; Luo, Y.; Fisher, S.; Fuller, J.; Edenson, S.; Lile, J.; Jarosinski, M. A.; Biere, A. L.; Curran, E.; Burgess, T.; Louis, J. C.; Collins, F.; Treanor, J.; Rogers, G.; Citron, M. β -secretase cleavage of Alzheimer's amyloid precursor protein by the transmembrane aspartic protease BACE. *Science* **1999**, *286*, 735–741. (c) Vassar, R.; Kovacs, D. M.; Yan, R.; Wong, P. C. The β -secretase enzyme in health and Alzheimer's disease: regulation, cell biology, function, and therapeutic potential. *J. Neurosci.* **2009**, *29*, 12787–12794.
- (4) (a) Luo, Y.; Bolon, B.; Kahn, S.; Bennett, B. D.; Babu-Khan, S.; Denis, P.; Fan, W.; Kha, H.; Zhang, J.; Gong, Y.; Martin, L.; Louis, J.-C.; Yan, Q.; Richards, W. G.; Citron, M.; Vassar, R. Mice deficient in BACE1, the Alzheimer's β -secretase, have normal phenotype and abolished β -amyloid generation. *Nat. Neurosci.* **2001**, *4*, 231–232. (b) Roberds, S. L.; Anderson, J.; Basi, G.; Bienkowski, M. J.; Branstetter, D. G.; Chen, K. S.; Freedman, S. B.; Frigon, N. L.; Games, D.; Hu, K.; Johnson-Wood, K.; Kappenman, K. E.; Kawabe, T. T.; Kola, I.; Kuehn, R.; Lee, M.; Liu, W.; Motter, R.; Nichols, N. F.; Power, M.; Robertson, D. W.; Schenk, D.; Schoor, M.; Shopp, G. M.; Shuck, M. E.; Sinha, S.; Svensson, K. A.; Tatsuno, G.; Tintrup, H.; Wijsman, J.; Wright, S.; McConlogue, L. BACE knockout mice are healthy despite lacking the primary β -secretase activity in brain: implications for Alzheimer's disease therapeutics. *Hum. Mol. Genet.* **2001**, *10*, 1317–1324.
- (5) (a) Citron, M. Alzheimer's disease: strategies for disease modification. *Nat. Rev. Drug Discovery* **2010**, *9*, 387–398. (b) Karran, E.; Mercken, M.; De Strooper, B. The amyloid cascade hypothesis for Alzheimer's disease: an appraisal for the development of therapeutics. *Nat. Rev. Drug Discovery* **2011**, *10*, 698–712.
- (6) (a) Rueeger, H.; Lueoend, R.; Rogel, O.; Rondeau, J.-M.; Mobitz, H.; Machauer, R.; Jacobson, L.; Staufenbiel, M.; Desrayaud, S.; Neumann, U. Discovery of cyclic sulfone hydroxyethylamines as potent and selective β -site APP-cleaving enzyme 1 (BACE1) inhibitors: structure-based design and in vivo reduction of amyloid β -peptides. *J. Med. Chem.* **2012**, *55*, 3364–3386. (b) Weiss, M. M.; Williamson, T.; Babu-Khan, S.; Bartberger, M. D.; Brown, J.; Chen, K.; Cheng, Y.; Citron, M.; Croghan, M. D.; Dineen, T. A.; Esmay, J.; Graceffa, R. F.; Harried, S. S.; Hickman, D.; Hitchcock, S. A.; Horne, D. B.; Huang, H.; Imbeah-Ampiah, R.; Judd, T.; Kaller, M. R.; Kreiman, C. R.; La, D. S.; Li, V.; Lopez, P.; Louie, S.; Monenschein, H.; Nguyen, T. T.; Pennington, L. D.; Rattan, C.; San Miguel, T.; Sickmier, E. A.; Wahl, R. C.; Wen, P. H.; Wood, S.; Xue, Q.; Yang, B. H.; Patel, V. F.; Zhong, W. Design and preparation of a potent series of hydroxyethylamine containing β -secretase inhibitors that demonstrate robust reduction of central β -amyloid. *J. Med. Chem.* **2012**, in press.
- (7) Cole, D. C.; Manas, E.; S.; Stock, J. R.; Condon, J. S.; Jennings, L. D.; Aulabaugh, A.; Chopra, R.; Cowling, R.; Ellingboe, J. W.; Fan, K. Y.; Harrison, B. L.; Hu, Y.; Jacobsen, S.; Jin, G.; Lin, L.; Lovering, F. E.; Malamas, M. S.; Stahl, J.; Strand, J.; Sukhedo, M. N.; Svenson, K.; Turner, M. J.; Wagner, E.; Wu, J.; Zhou, P.; Bard, J. Acylguanidines as small-molecule β -secretase inhibitors. *J. Med. Chem.* **2006**, *49*, 6158–6161.
- (8) Malamas, M. S.; Erdei, J.; Gunawan, I.; Barnes, K.; Johnson, M.; Hui, Y.; Turner, J.; Hu, Y.; Wagner, E.; Fan, K.; Olland, A.; Bard, J.; Robichaud, A. J. Aminoimidazoles as potent and selective human β -secretase (BACE1) inhibitors. *J. Med. Chem.* **2009**, *52*, 6314–6323.
- (9) Baxter, E. W.; Conway, K. A.; Kennis, L.; Bischoff, F.; Mercken, M. H.; Winter, H. L.; Reynolds, C. H.; Tounge, B. A.; Luo, C.; Scott, M. K.; Huang, Y.; Braeken, M.; Pieters, S. M.; Berthelot, D. J.; Masure, S.; Bruinzeel, W. D.; Jordan, A. D.; Parker, M. H.; Boyd, R. E.; Qu, J.; Alexander, R. S.; Breneman, D. E.; Reitz, A. B. 2-Amino-3,4-dihydroquinazolines as inhibitors of BACE-1 (β -site APP cleaving enzyme): use of structure based design to convert a micromolar hit into a nanomolar lead. *J. Med. Chem.* **2007**, *50*, 4261–4264.
- (10) (a) Zhu, Z.; Sun, Z.-Y.; Ye, Y.; Voigt, J.; Strickland, C.; Smith, E. M.; Cumming, J.; Wang, L.; Wong, J.; Wang, Y.-S.; Wyss, D. F.; Chen, X.; Kuvelkar, R.; Kennedy, M. E.; Favreau, L.; Parker, E.; McKittrick, B. A.; Stamford, A.; Czarniecki, M.; Greenlee, W.; Hunter, J. C. Discovery of cyclic acylguanidines as highly potent and selective β -site amyloid cleaving enzyme (BACE) inhibitors: part I—inhibitor design and validation. *J. Med. Chem.* **2010**, *53*, 951–965. (b) Berg, S.; Burrows, J.; Chessari, G.; Congreve, M. S.; Hedström, J.; Hellberg, S.; Högdin, K.; Kihlström, J.; Kolmodin, K.; Lindström, J.; Murray, C.; Patel, S. Novel 2-amino-imidazole-4-one compounds and their use in the manufacture of a medicament to be used in the treatment of cognitive impairment, Alzheimer's disease, neurodegeneration and dementia. Patent WO2007058602, 2007.
- (11) Congreve, M.; Aharon, D.; Albert, J.; Callaghan, O.; Campbell, J.; Carr, R. A. E.; Chessari, G.; Cowan, S.; Edwards, P. D.; Frederickson, M.; McMenamin, R.; Murray, C. W.; Patel, S.; Wallis, N. Application of fragment screening by X-ray crystallography to the discovery of aminopyridines as inhibitors of β -secretase. *J. Med. Chem.* **2007**, *50*, 1124–1132.
- (12) Edwards, P. D.; Albert, J. S.; Sylvester, M.; Aharon, D.; Andisik, D.; Callaghan, O.; Campbell, J. B.; Carr, R. A.; Chessari, G.; Congreve, M.; Frederickson, M.; Folmer, R. H.; Geschwindner, S.; Koether, G.; Kolmodin, K.; Krumrine, J.; Mauger, R. C.; Murray, C. W.; Olsson, L.-L.; Patel, S.; Spear, N.; Tian, G. Application of fragment-based lead generation to the discovery of novel, cyclic amidine β -secretase inhibitors with nanomolar potency, cellular activity, and high ligand efficiency. *J. Med. Chem.* **2007**, *50*, 5912–5925.
- (13) Cheng, Y.; Judd, T. C.; Bartberger, M. D.; Brown, J.; Chen, K.; Freneau, R. T.; Hickman, D.; Hitchcock, S. A.; Jordan, B.; Li, V.; Lopez, P.; Louie, S. W.; Luo, Y.; Michelsen, K.; Nixey, T.; Powers, T. S.; Rattan, C.; Sickmier, E. A.; St; Jean, D. J., Jr.; Wahl, R. C.; Wen, P. H.; Wood, S. From fragment screening to in vivo efficacy: optimization of a series of 2-aminoquinolines as potent inhibitors of β -site amyloid precursor protein cleaving enzyme 1 (BACE1). *J. Med. Chem.* **2011**, *54*, 5836–5857.
- (14) (a) Stanton, M. G.; Stauffer, S. R.; Gregro, A. R.; Steinbeiser, M.; Nantermet, P.; Sankaranarayanan, S.; Price, E. A.; Wu, G.; Crouthamel, M.-C.; Ellis, J.; Lai, M.-T.; Espeseth, A. S.; Shi, X.-P.; Jin, L.; Colussi, D.; Pietrak, B.; Huang, Q.; Xu, M.; Simon, A. J.; Graham, S. L.; Vacca, J. P.; Selnick, H. Discovery of isonicotinamide derived β -secretase inhibitors: in vivo reduction of β -amyloid. *J. Med. Chem.* **2007**, *50*, 3431–3433. (b) Sankaranarayanan, S.; Holahan, M. A.; Colussi, D.; Crouthamel, M.-C.; Devanarayan, V.; Ellis, J.; Espeseth, A.; Gates, A. T.; Graham, S. L.; Gregro, A. R.; Hazuda, D.; Hochman, J. H.; Holloway, K.; Jin, L.; Kahana, J.; Lai, M.-T.; Lineberger, J.; McGaughey, G.; Moore, K. P.; Nantermet, P.; Pietrak, B.; Price, E. A.; Rajapakse, H.; Stauffer, S.; Steinbeiser, M. A.; Seabrook, G.; Selnick, H. G.; Shi, X.-P.; Stanton, M. G.; Swestock, J.; Tugusheva, K.; Tyler, K. X.; Vacca, J. P.; Wong, J.; Wu, G.; Xu, M.; Cook, J. J.; Simon, A. J. First demonstration of cerebrospinal fluid and plasma A β lowering with oral

- administration of a β -site amyloid precursor protein-cleaving enzyme 1 inhibitor in nonhuman primates. *J. Pharmacol. Exp. Ther.* **2009**, *328*, 131–140. (c) Zhu, H.; Young, M. B.; Nantermet, P. G.; Graham, S. L.; Colussi, D.; Lai, M.-T.; Pietrak, B.; Price, E. A.; Sankaranarayanan, S.; Shi, X. P.; Tugusheva, K.; Holahan, M. A.; Michener, M. S.; Cook, J. J.; Simon, A.; Hazuda, D. J.; Vacca, J. P.; Rajapakse, H. A. Rapid P1 SAR of brain penetrant tertiary carbinamine derived BACE inhibitors. *Bioorg. Med. Chem. Lett.* **2010**, *20*, 1779–1782. (d) Cumming, J. N.; Smith, E. M.; Wang, L.; Misiaszek, J.; Durkin, J.; Pan, J.; Iserloh, U.; Wu, Y.; Zhu, Z.; Strickland, C.; Voigt, J.; Chen, X.; Kennedy, M. E.; Kuvelkar, R.; Hyde, L. A.; Cox, K.; Favreau, L.; Czarniecki, M. F.; Greenlee, W. J.; McKittrick, B. A.; Parker, E. M.; Stamford, A. W. Structure based design of iminohydantoin BACE1 inhibitors: identification of an orally available, centrally active BACE1 inhibitor. *Bioorg. Med. Chem. Lett.* **2012**, *22*, 2444–2449.
- (15) May, P. C.; Dean, R. A.; Lowe, S. L.; Martenyi, F.; Sheehan, S. M.; Boggs, L. N.; Monk, S. A.; Mathes, B. M.; Mergott, D. J.; Watson, B. M.; Stout, S. L.; Timm, D. E.; Smith Labell, E.; Gonzales, C. R.; Nakano, M.; Jhee, S. S.; Yen, M.; Ereshefsky, L.; Lindstrom, T. D.; Calligaro, D. O.; Cocke, P. J.; Hall, G. D.; Friedrich, S.; Citron, M.; Audia, J. E. Robust central reduction of amyloid- β in humans with an orally available, non-peptidic β -secretase inhibitor. *J. Neurosci.* **2011**, *31*, 16507–16516.
- (16) Swahn, B.-M.; Holenz, J.; Kihlström, J.; Kolmodin, K.; Lindström, J.; Plobeck, N.; Rotticci, D.; Sehgelmeble, F.; Sundström, M.; von Berg, S.; Färling, J.; Georgievska, B.; Gustavsson, S.; Neelissen, J.; Ek, M.; Olsson, L.-L.; Berg, S. Aminoimidazoles as BACE-1 inhibitors: the challenge to achieve in vivo brain efficacy. *Bioorg. Med. Chem. Lett.* **2012**, *22*, 1854–1859.
- (17) Roden, D. M. Drug-induced prolongation of the QT interval. *N. Engl. J. Med.* **2004**, *350*, 1013–1022.
- (18) Vik, T.; Pollard, C.; Sager, P. Early clinical development: evaluation of drug-induced torsades de pointes risk. *Pharmacol Ther.* **2008**, *119*, 210–214.
- (19) Miyaura, N.; Suzuki, A. Palladium-catalyzed cross-coupling reactions of organoboron compounds. *Chem. Rev.* **1995**, *95*, 2457–2483.
- (20) Malamas, M. S.; Erdei, J.; Gunawan, I.; Turner, J.; Hu, Y.; Wagner, E.; Fan, K.; Chopra, R.; Olland, A.; Bard, J.; Jacobsen, S.; Magolda, R. L.; Pangalos, M.; Robichaud, A. J. Design and synthesis of 5,5'-disubstituted aminohydantoins as potent and selective human β -secretase (BACE1) inhibitors. *J. Med. Chem.* **2010**, *53*, 1146–1158.
- (21) Hong, L.; Koelsch, G.; Lin, X. L.; Wu, S. L.; Terzyan, S.; Ghosh, A. K.; Zhang, X. C.; Tang, J. Structure of the protease domain of memapsin 2 (β -secretase) complexed with inhibitor. *Science* **2000**, *290*, 150–153.
- (22) Cumming, J. G.; Tucker, H.; Oldfield, J.; Fielding, C.; Highton, A.; Faull, A.; Wild, M.; Brown, D.; Wells, S.; Shaw, J. Balancing hERG affinity and absorption in the discovery of AZD5672, an orally active CCR5 antagonist for the treatment of rheumatoid arthritis. *Bioorg. Med. Chem. Lett.* **2012**, *22*, 1655–1659.
- (23) (a) Leeson, P. D.; Empfield, J. R. Reducing the risk of drug attrition associated with physicochemical properties. *Annu. Rep. Med. Chem.* **2010**, *45*, 393–407. (b) Waring, M. J. Lipophilicity in drug discovery. *Expert Opin. Drug Discovery* **2010**, *5*, 235–248.
- (24) Adams, J. L.; Boehm, J. C.; Kassis, S.; Gorycki, P. D.; Webb, E. F.; Hall, R.; Sorenson, M.; Lee, J. C.; Ayrton, A.; Griswold, D. E.; Gallagher, T. F. Pyrimidinylimidazole inhibitors of CSBP/p38 kinase demonstrating decreased inhibition of hepatic cytochrome P450 enzymes. *Bioorg. Med. Chem. Lett.* **1998**, *8*, 3111–3116.
- (25) (a) Stachel, S. J.; Coburn, C. A.; Rush, D.; Jones, K. L. G.; Zhu, H.; Rajapakse, H.; Graham, S. L.; Simon, A.; Holloway, M. K.; Allison, T. J.; Munshi, S. K.; Espeseth, A. S.; Zuck, P.; Colussi, D.; Wolfe, A.; Pietrak, B. L.; Lai, M.-T.; Vacca, J. P. Discovery of aminoheterocycles as a novel β -secretase inhibitor class: pH dependence on binding activity part 1. *Bioorg. Med. Chem. Lett.* **2009**, *19*, 2977–2980. (b) Dominguez, J. L.; Christopheit, T.; Villaverde, M. C.; Gossas, T.; Otero, J. M.; Nystrom, S.; Baraznenok, V.; Lindstrom, E.; Danielson, U. H.; Sussman, F. Effect of the protonation state of the titratable residues on the inhibitor affinity to BACE-1. *Biochemistry* **2010**, *49*, 7255–7263.
- (26) (a) Bridgland-Taylor, M. H.; Hargreaves, A. C.; Easter, A.; Orme, A.; Henthorn, D. C.; Ding, M.; Davis, A. M.; Small, B. G.; Heapy, C. G.; Abi-Gerges, N.; Persson, F.; Jacobson, I.; Sullivan, M.; Albertson, N.; Hammond, T. G.; Sullivan, E.; Valentin, J. P.; Pollard, C. E. Optimisation and validation of a medium-throughput electrophysiology-based hERG assay using IonWorks HT. *J. Pharmacol. Toxicol. Methods* **2006**, *54*, 189–199. (b) Schroeder, K.; Neagle, B.; Trezise, D. J.; Worley, J. IonWorks: a new high-throughput electrophysiology measurement platform. *J. Biomol. Screening* **2003**, *8*, 50–64.
- (27) (a) Floby, E.; Briem, S.; Terelius, Y.; Sohlenius-Sternbeck, A.-K. The use of a cocktail of probe substrates for drug-metabolizing enzymes for the assessment of the metabolic capacity of hepatocyte preparations. *Xenobiotica* **2004**, *34*, 949–959. (b) Bissell, D. M.; Guzelian, P. S. Phenotypic stability of adult rat hepatocytes in primary monolayer culture. *Ann. N. Y. Acad. Sci.* **1980**, *249*, 85–98.
- (28) (a) Wan, H.; Holmén, A.; Wang, Y. D.; Lindberg, W.; Englund, M.; Någård, M.; Thompson, R. High throughput screening of pKa values of pharmaceuticals by pressure-assisted capillary electrophoresis and mass spectrometry. *Rapid Commun. Mass Spectrom.* **2003**, *1*, 2639–2648. (b) Wan, H.; Holmén, A.; Någård, M.; Lindberg, W. Rapid screening of pKa values of pharmaceuticals by pressure-assisted capillary electrophoresis combined with short-end injection. *J. Chromatogr., A* **2002**, *979*, 369–377.
- (29) Lombardo, F.; Shalaeva, M. Y.; Tupper, K. A.; Gao, F. ElogD_{oc}: a tool for lipophilicity determination in drug discovery. 2. Basic and neutral compounds. *J. Med. Chem.* **2001**, *44*, 2490–2497.
- (30) (a) Laurence, C.; Brameld, K. A.; Graton, J.; Le Questel, J.-Y.; Renault, E. The pKBHX Database: toward a better understanding of hydrogen-bond basicity for medicinal chemists. *J. Med. Chem.* **2009**, *52*, 4073–4086. (b) Bissantz, C.; Kuhn, B.; Stahl, M. A medicinal chemist's guide to molecular interactions. *J. Med. Chem.* **2010**, *53*, 5061–5084.
- (31) (a) Zhou, P.; Li, Y.; Fan, Y.; Wang, Z.; Chopra, R.; Olland, A.; Hu, Y.; Magolda, R. L.; Pangalos, M.; Reinhart, P. H.; Turner, M. J.; Bard, J.; Malamas, M. S.; Robichaud, A. J. Pyridinyl aminohydantoins as small molecule BACE1 inhibitors. *Bioorg. Med. Chem. Lett.* **2010**, *20*, 2326–2329. (b) Malamas, M. S.; Robichaud, A.; Erdei, J.; Quagliato, D.; Solvibile, W.; Zhou, P.; Morris, K.; Turner, J.; Wagner, E.; Fan, K.; Olland, A.; Jacobsen, S.; Reinhart, P.; Riddell, D.; Pangalos, M. Design and synthesis of aminohydantoins as potent and selective human β -secretase (BACE1) inhibitors with enhanced brain permeability. *Bioorg. Med. Chem. Lett.* **2010**, *20*, 6597–6605.
- (32) Patel, S.; Vuillard, L.; Cleasby, A.; Murray, C. W.; Yon, J. Apo and inhibitor complex structures of BACE (β -secretase). *J. Mol. Biol.* **2004**, *343*, 407–416.
- (33) Laskowski, R. A.; MacArthur, M. W.; Moss, D. S.; Thornton, J. M. PROCHECK: a program to check the stereochemical quality of protein structures. *J. Appl. Crystallogr.* **1993**, *26*, 283–291.
- (34) (a) Borgegård, T.; Minidis, A.; Juréus, A.; Malmberg, J.; Rosqvist, S.; Gruber, S.; Almqvist, H.; Yan, H.; Bogstedt, A.; Olsson, F.; Dahlström, J.; Ray, C.; Närhi, K.; Malinowsky, D.; Hagström, E.; Jin, S.; Malmberg, A.; Lendahl, U.; Lundkvist, J. In vivo analysis using a presenilin-1-specific inhibitor. Presenilin-1-containing γ -secretase complexes mediate the majority of CNS A β production in the mouse. *Alzheimer Dis. Res. J.* **2011**, *3*, 29–45. (b) Friden, M.; Gupta, A.; Antonsson, M.; Bredberg, U.; Hammarlund-Udenaes, M. *In vitro* methods for estimating unbound drug concentrations in the brain interstitial and intracellular fluids. *Drug Metab. Dispos.* **2007**, *35*, 1711.
- (35) Leslie, A. G. W. Recent changes to the MOSFLM package for processing film and image plate data. *Joint CCP4 + ESRF-EAMCB News. Protein Crystallogr.* **1992**, No. 26.
- (36) Collaborative Computational Project, number 4. The CCP4 suite: programs for protein crystallography. *Acta Crystallogr., Sect. D: Biol. Crystallogr.* **1994**, *D50*, 760–763.
- (37) Vonrhein, C.; Flensburg, C.; Keller, P.; Sharff, A.; Smart, O. S.; Paciorek, W.; Womack, T. O.; Bricogne, G. Data processing and

analysis with the autoPROC toolbox. *Acta Crystallogr., Sect. D: Biol. Crystallogr.* **2011**, *D67*, 293–302.

(38) Kabsch, W. XDS. *Acta Crystallogr., Sect. D: Biol. Crystallogr.* **2010**, *D66*, 125–132.

(39) Murshudov, G. N.; Vagin, A. A.; Dodson, E. J. Refinement of macromolecular structures by the maximum-likelihood method. *Acta Crystallogr., Sect. D: Biol. Crystallogr.* **1997**, *D53*, 240–255.

(40) Bricogne, G.; Blanc, E.; Brandl, M.; Flensburg, C.; Keller, P.; Paciorek, W.; Roversi, P.; Sharff, A.; Smart, O. S.; Vonrhein, C.; Womack, T. O. *BUSTER*, version 2.11.1; Global Phasing Ltd.: Cambridge, U.K., 2011.

(41) Emsley, P.; Cowtan, K. Coot: model-building tools for molecular graphics. *Acta Crystallogr., Sect. D: Biol. Crystallogr.* **2004**, *D60*, 2126–2132.

(42) Delano, W. L. *The PyMOL Molecular Graphics System*; Delano Scientific: Palo Alto, CA, 2002.

■ NOTE ADDED AFTER ASAP PUBLICATION

After this paper was published online September 17, 2012, author Fredrik von Kieseritzky was added to the author list. The corrected version was reposted October 3, 2012.